Production of Ξ^{-} hypernuclei and properties of Ξ-nucleus potentials

T. Harada

Osaka Electro-Communication Univ.
/J-PARC Branch, KEK Theory Center

Collaboration with Y. Hirabayashi (Hokkaido Univ.)

Outline

1. Introduction
   - Theoretical studies of Ξ^- s.p. potentials
   - Experimental information on Ξ^- hypernuclei
2. Production of Ξ^- hypernuclei
   - Distorted-wave Impulse approximation (DWIA)
   - Medium effects on Ξ^- production Optimal Fermi averaging (OFA)
   - Analysis of Ξ^- QF spectra of the $^{9}Be(K^{-}, K^{+})$ reaction
   - Properties of the Ξ^--^{8}Li potential
3. Properties of Ξ-nucleus potentials
   - Ξ^--^{12}C vs. Ξ^--^{14}N potentials
   - Ξ^--^{56}Fe potentials and Ξ^--atomic states
   - Discussion
4. Summary

1. Introduction

Theoretical studies of Ξ^- s.p. potentials

V_Ξ ?

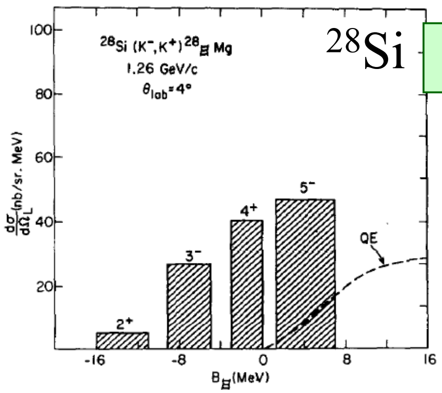

Ξ-hypernuclei via (K-,K+) reactions

C.B. Dover, A.Gal, Ann. Phys. 146 (1989) 309.

$$V_\Xi^0 = -24 \pm 4 \text{ MeV} \quad \text{for} \quad r_0 = 1.1 \text{ fm} \quad (W_\Xi^0 \simeq -1 \text{ MeV})$$

DWIA analysis of ^{12}C(K-,K+) spectra from BNL exp.

T.Iijima et al.,NPA546(1992) 588.
Tadokoro et al., PRC51(1995) 2656

$$V_\Xi^0 \simeq -16 \text{ MeV}$$

P.Khaustov et al., PRC61(2000) 054603

$$V_\Xi^0 \simeq -14 \text{ MeV}$$

↓

Ehime, ESC16a/b, HAL (Yamamoto)

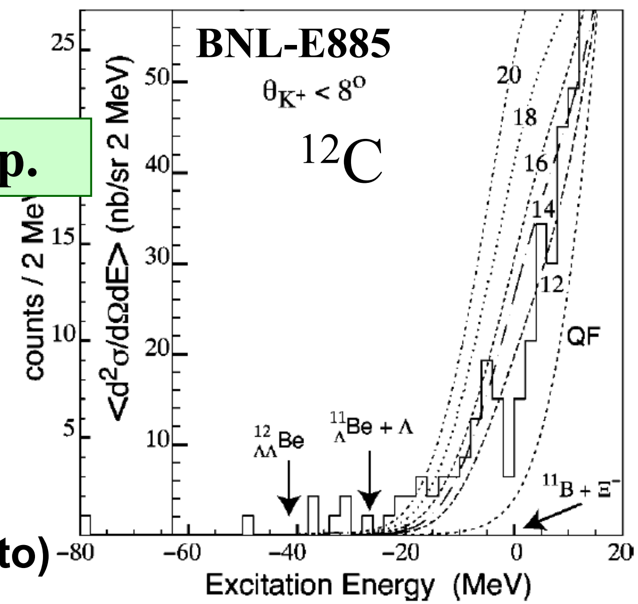

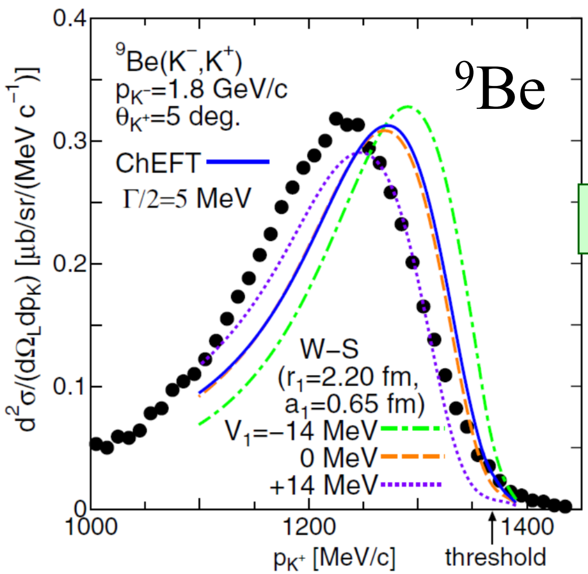

Semi-Classical Distorted Wave Model Analysis

M. Kohno et al.,PTP123(2010)157; NPA835(2010)358.

$$V_\Xi^0 = -20, -10, 0, +10, +20\text{MeV}$$ **(fss2)**

M. Kohno, PRC100 (2019) 024313

$$V_\Xi^0 = -14, 0, +14 \quad \text{MeV}$$ **(Chiral NLO)**

Experimental Information on Ξ^- Hypernuclei

"KISO" event from emulsion

Nakazawa, et al., PTEP, 2015, 033D02

$$\Xi^- + {}^{14}\mathrm{N} \rightarrow {}^{10}_{\Lambda}\mathrm{Be}(\#1) + {}^{5}_{\Lambda}\mathrm{He}(\#2)$$

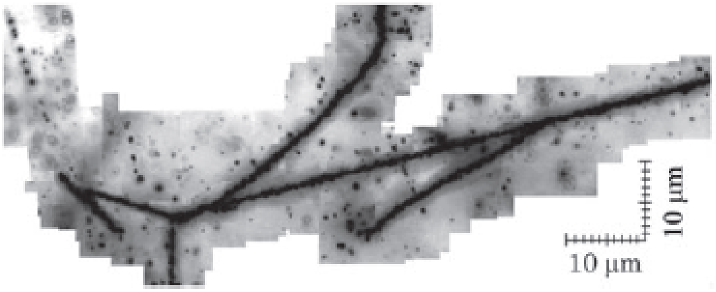

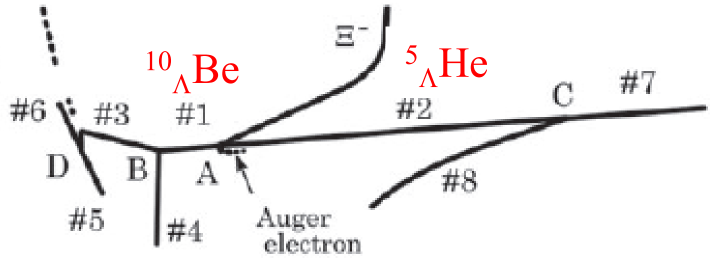

B_{Ξ} (2p) = 1.03 ±0.18 MeV or 3.87 ±0.21 MeV, which suggested to form a Coulomb-assisted nuclear 2p bound state for Ξ–.

^{12}C(K–,K+)$^{12}{}_{\Xi}$Be spectrum in J-PARC E05

T. Nagae et al., AIP Conf. Proc. 2130, 020015 (2019).

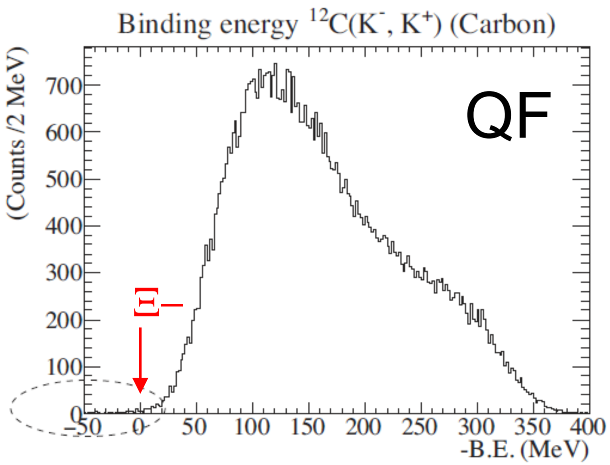

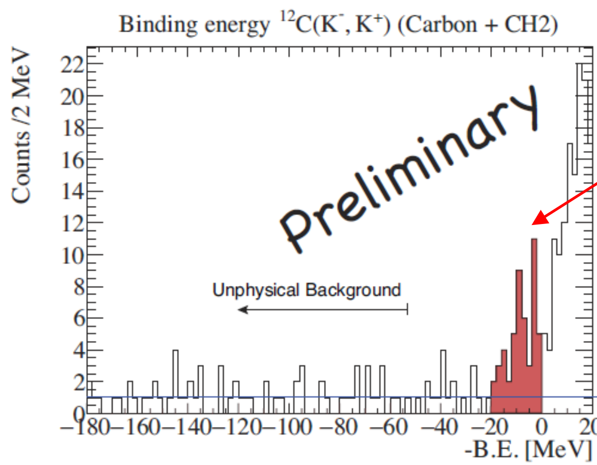

Ξ– bound state evidence

5.4 MeV FWHM

✓ Accurate observation of Ξ^- production: Their analysis is now ongoing.

Recent observations of Ξ^- hypernuclei from emulsion compared with theoretical predictions

$\Xi^- + {}^{14}N$

M. Yoshimoto, Prog. Theor. Exp. Phys. **2021**, 073D02.

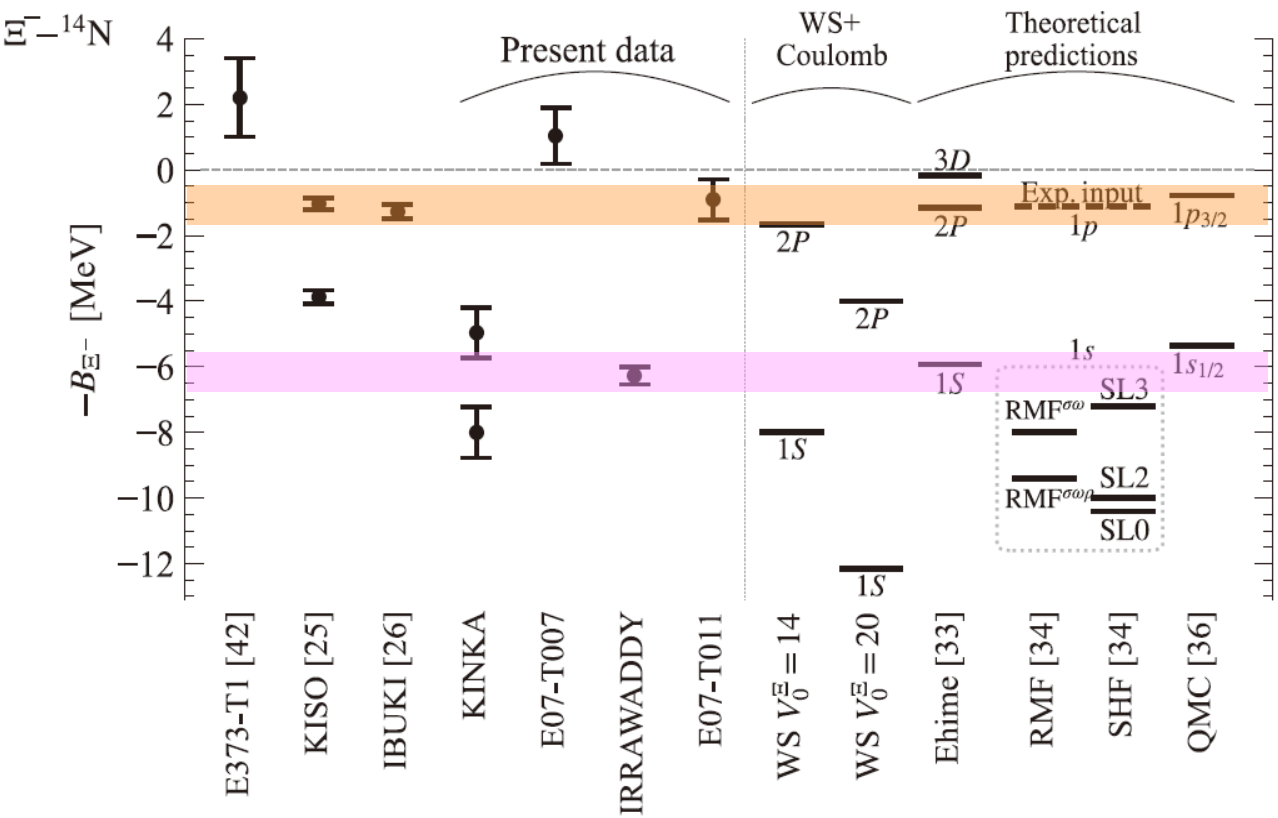

2P capture

1s?

Coulomb only in $\Xi^-{}^{14}N$:
B_Ξ(2P)= 0.39 MeV
B_Ξ(1s)= 1.21 MeV

✓ Ξ^- capture from the 2P state: B_Ξ (2P) = 1.03 MeV(KISO)-1.27 MeV (IBUKI)
- The Ξ-nucleus potential is attractive in the real part.
- The 2P capture rate (4%) obtained from cascade cal.
  → ΞN-ΛΛ coupling is weak (consistent with HAL-QCD).

In this talk,

We study theoretically production of Ξ^- hypernuclei in the nuclear (K^-, K^+) reaction and properties of the Ξ-nucleus potential.

- We evaluate the in-medium cross sections of the $K^- p \to K^+ \Xi^-$ reaction, using the optimal Fermi-averaging procedure (OFA). T. Harada and Y. Hirabayashi, PRC102 (2020) 024618.
- We demonstrate the Ξ^- QF spectrum produced via the ^{9}Be(K^-, K^+) reaction at 1.8 GeV/c to extract useful information on the Ξ-nucleus potential for Ξ^--^{8}Li from the data of the BNL-E906 experiment.
  T. Harada and Y. Hirabayashi, PRC103 (2021) 024605.
- We discuss the properties of Ξ-nucleus potentials in comparison with the recent data from emulsion.

2. Production of Ξ^- hypernuclei

2.1
Distroted wave impulse approximation (DWIA)

Distorted-wave impulse approximation (DWIA)

- Inclusive double-differential cross sections

$$\frac{d^2\sigma}{dE_{K^+}d\Omega_{K^+}} = \beta\frac{1}{[J_A]}\sum_{m_A}\sum_{B,m_B}|\langle\Psi_B|\hat{F}|\Psi_A\rangle|^2\,\delta(\omega - E_B + E_A)$$

- Energy transfer and momentum transfer in lab. system

$$\omega = E_{K^-} - E_{K^+}, \qquad \boldsymbol{q} = \boldsymbol{p}_{K^-} - \boldsymbol{p}_{K^+}$$

- Kinematical factor for translating from K-N to K-A.

$$\beta = \left(1 + \frac{E_{K^+}^{(0)}}{E_B^{(0)}}\frac{p_{K^+}^{(0)} - p_{K^-}^{(0)}\cos\theta_{\rm lab}}{p_{K^+}^{(0)}}\right)\frac{p_{K^+}E_{K^+}}{p_{K^+}^{(0)}E_{K^+}^{(0)}}$$

- External operator for the production reaction

$$\hat{F} = \int d\boldsymbol{r}\,\chi_{\boldsymbol{p}_{K^+}}^{(-)*}(\boldsymbol{r})\chi_{\boldsymbol{p}_{K^-}}^{(+)}(\boldsymbol{r})\sum_{j=1}^{A}\overline{f}_{K^-p\to K^+\Xi^-}\,\delta(\boldsymbol{r} - \boldsymbol{r}_j)\hat{O}_j$$

Distorted-waves for outgoing K^+ and incoming K^-

Eikonal approximation

C. B. Dover, et al., PRC**22**, 2073 (1980).

$$\chi_K^{(-)*}(\boldsymbol{r})\chi_{K^-}^{(+)}(\boldsymbol{r}) = \exp(i\boldsymbol{q}\cdot\boldsymbol{r})D(\boldsymbol{b},z)$$

$$D(\boldsymbol{b},z) = \exp\left(-\frac{\sigma_{K^-}(1-i\alpha_{K^-})}{2}\int_{-\infty}^{z}\rho(\boldsymbol{b},z')\,dz' - \frac{\sigma_K(1+i\alpha_K)}{2}\int_{z}^{\infty}\rho(\boldsymbol{b},z')\,dz'\right)$$

$$\sigma_m = (Z/A)\sigma_{mp}^{\text{tot}} + (N/A)\sigma_{mn}^{\text{tot}} \qquad \alpha_{K^-} = \alpha_K = 0$$

$$\sigma_{K^-} = 28.9 \text{ mb} \qquad \sigma_{K^+} = 19.4 \text{ mb}$$

T. Motoba, et al., PRC**38**, 1322 (1988).
S. Tadokoro, et al., PRC**51**, 2656 (1995).
P. Khaustov et al., PRC**61**, 054603 (2000).

Partial wave expansion

$$\chi_K^{(-)*}(\boldsymbol{r})\chi_{K^-}^{(+)}(\boldsymbol{r}) = \sum_L \sqrt{4\pi(2L+1)}\, i^L \tilde{j}_L(r) Y_L^0(\hat{\boldsymbol{r}})$$

$$\tilde{j}_L(r) = \sum_{\ell\ell'}\sqrt{\frac{2\ell'+1}{4\pi}}\frac{2\ell+1}{2L+1} i^{\ell-L}(\ell 0 \ell' 0|L0)^2 j_\ell(r) D_{\ell'}(r)$$

$\ell \leqslant 30$ Recoil effect: $\boldsymbol{r} \to \frac{M_C}{M_A}\boldsymbol{r}$

Production cross sections in A(a,b)$_Y$B reacrions

Morimatsu, Yazaki, NPA483 (1988) 493.

Green's function method

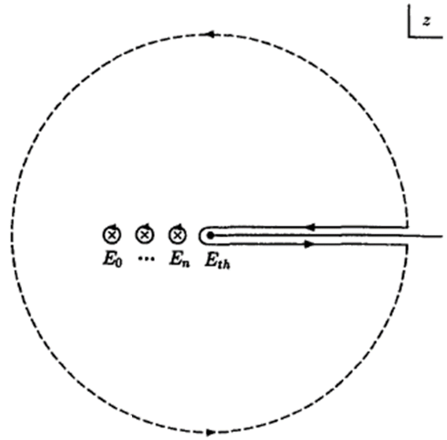

- Strength function

$$S(E) = \sum_{B,m_B} |\langle \Psi_B | \hat{F} | \Psi_A \rangle|^2 \delta(\omega - E_B + E_A)$$

$$= -\frac{1}{\pi} \mathrm{Im} \sum_{\alpha\alpha'} \int d\boldsymbol{r} d\boldsymbol{r}' F_{\Xi}^{\alpha\,\dagger}(\boldsymbol{r}) G_{\Xi}^{\alpha\alpha'}(E; \boldsymbol{r}, \boldsymbol{r}') F_{\Xi}^{\alpha'}(\boldsymbol{r}')$$

$$\sum_B |\Psi_B\rangle \delta(E - E_B) \langle \Psi_B| = (-)\frac{1}{\pi} \mathrm{Im}\left[\frac{1}{E - H_B + i\epsilon}\right]$$

- Completeness relation

$$G^{(+)}(E; \boldsymbol{r}, \boldsymbol{r}') = \sum_n \frac{\varphi_n(\boldsymbol{r})(\tilde{\varphi}_n(\boldsymbol{r}'))^*}{E - E_n + i\epsilon} + \frac{2}{\pi}\int_0^\infty dk \frac{k^2 S(k) u(k, \boldsymbol{r})(\tilde{u}(k, \boldsymbol{r}'))^*}{E - E_k + i\epsilon}$$

bound states,
quasibound states

Continuum states,
resonance states

2.2
Medium effects on Ξ^- production

Distorted-wave impulse approximation (DWIA)

- Inclusive double-differential cross sections

$$\frac{d^2\sigma}{dE_{K^+}d\Omega_{K^+}} = \beta \frac{1}{[J_A]} \sum_{m_A} \sum_{B,m_B} |\langle \Psi_B | \hat{F} | \Psi_A \rangle|^2 \delta(\omega - E_B + E_A)$$

- Energy transfer and momentum transfer in lab. system

$$\omega = E_{K^-} - E_{K^+}, \qquad \boldsymbol{q} = \boldsymbol{p}_{K^-} - \boldsymbol{p}_{K^+}$$

- Kinematical factor for translating from K-N to K-A.

$$\beta = \left(1 + \frac{E_{K^+}^{(0)}}{E_B^{(0)}} \frac{p_{K^+}^{(0)} - p_{K^-}^{(0)} \cos\theta_{\rm lab}}{p_{K^+}^{(0)}} \right) \frac{p_{K^+} E_{K^+}}{p_{K^+}^{(0)} E_{K^+}^{(0)}}$$

- External operator for the production reaction

$$\hat{F} = \int d\boldsymbol{r}\, \chi_{\boldsymbol{p}_{K^+}}^{(-)*}(\boldsymbol{r}) \chi_{\boldsymbol{p}_{K^-}}^{(+)}(\boldsymbol{r}) \sum_{j=1}^{A} \overline{f}_{K^- p \to K^+ \Xi^-} \delta(\boldsymbol{r} - \boldsymbol{r}_j) \hat{O}_j$$

↖ In-medium $K^- p \to K^+ \Xi^-$ amplitude

Differential cross sections for the $K^- p \to K^+ \Xi^-$ reactions

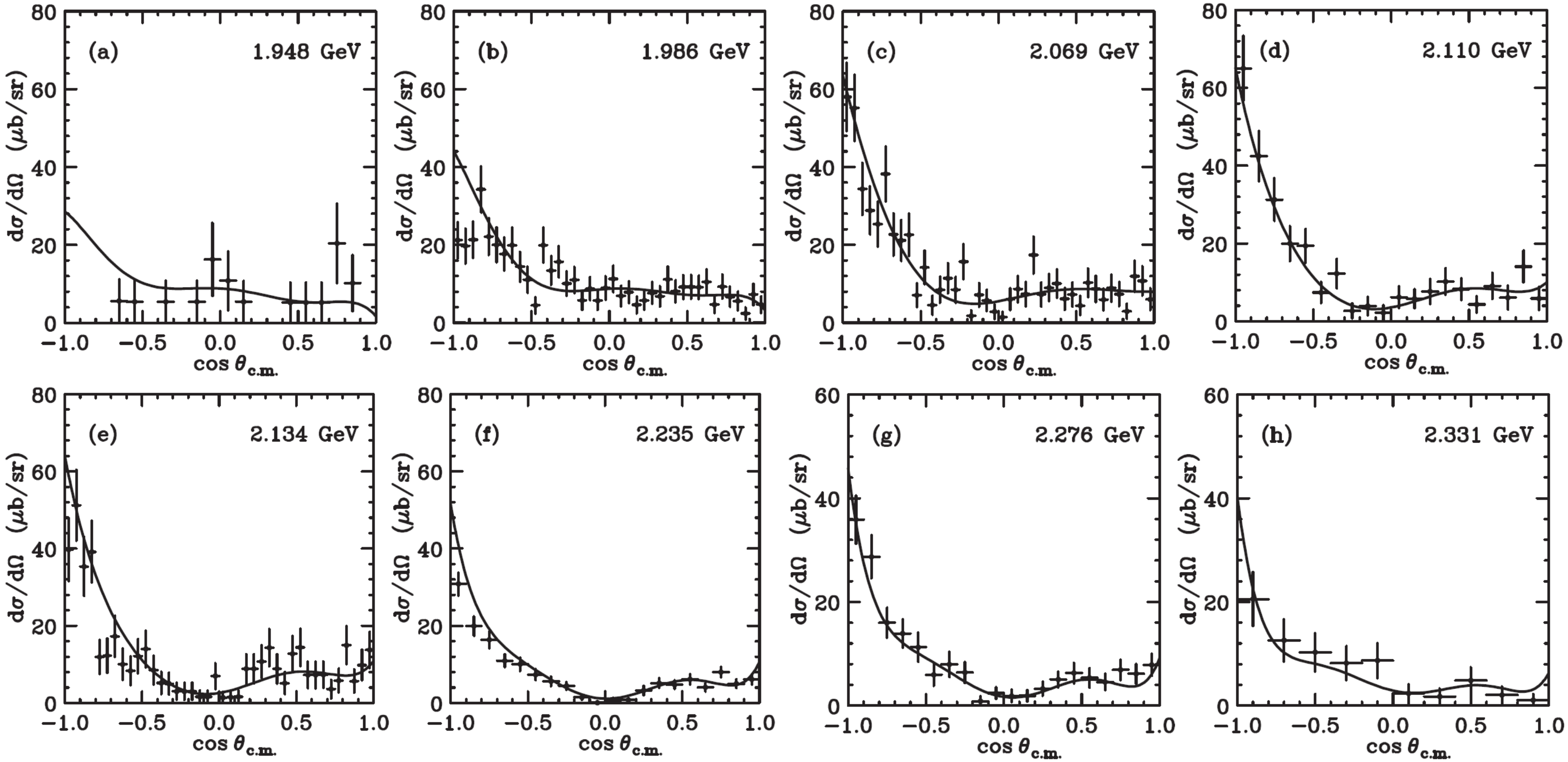

free space

Experimental data :

W. P. Trower, et al., PR170, 1207 (1968).
G. Burgun et al., NPB 8, 447 (1968).
P. M. Dauber, et al., PR179, 1262 (1969).
T. G. Trippe and P. E. Schlein, PR158, 1334 (1967).
G. W. London, et al., PR143, 1034 (1966).
V. Flaminio, et al., CERN-HERA Report 79-02 (1979).

$$\left(\frac{d\sigma}{d\Omega}\right)^{\mathrm{elem}}_{\mathrm{c.m.}} = \lambda\!\!\!^{-}{}^2 \sum_{\ell=0}^{\ell_{\max}} A_\ell(E_{\mathrm{c.m.}}) P_\ell(\cos\theta_{\mathrm{c.m.}})$$

Parameters ($\ell \leq 6$) for fits to the data

Total cross section σ_{tot} for the $K^{-}p \rightarrow K^{+}\Xi^{-}$ reaction

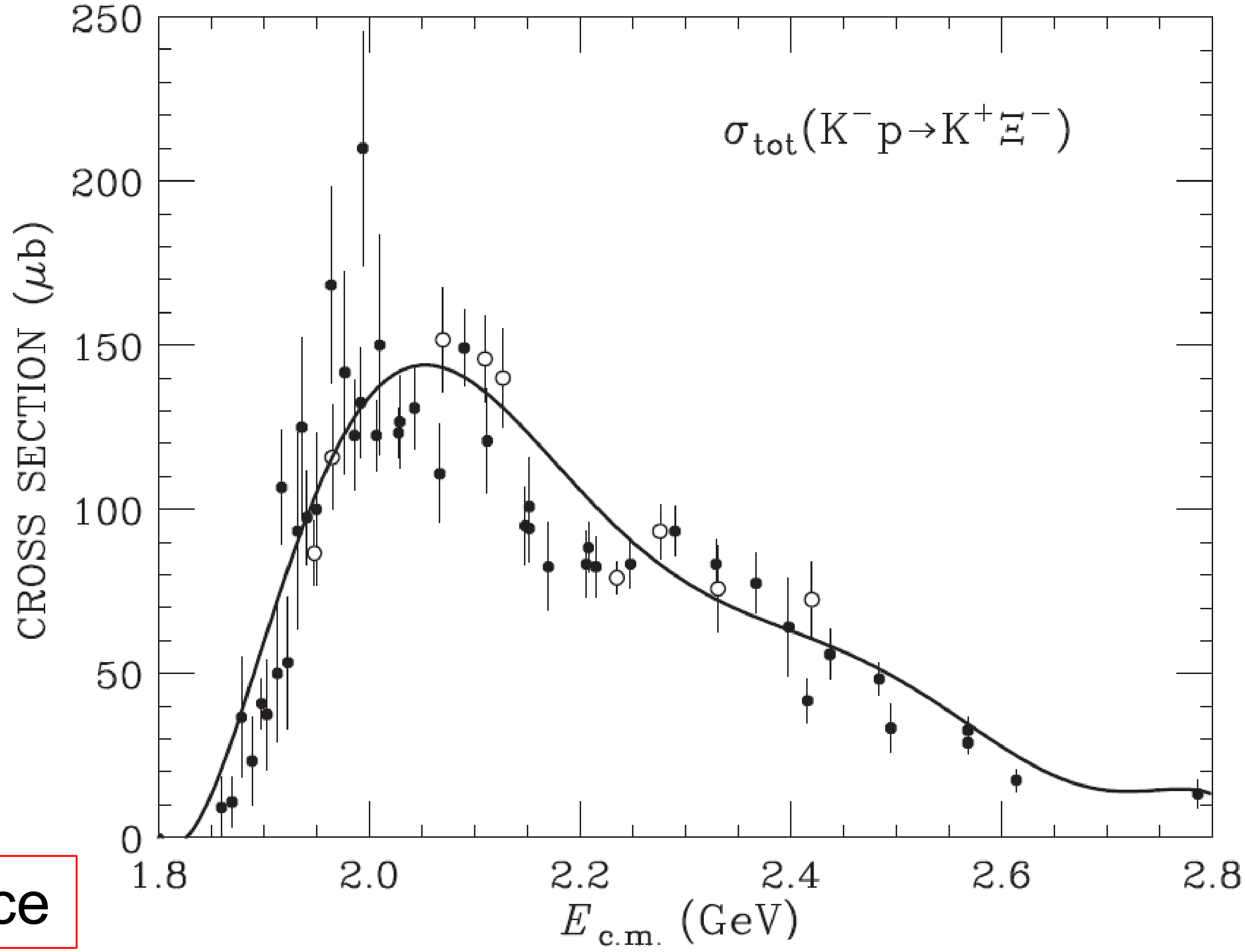

free space

Data taken from

V. Flaminio, et al., CERN-HERA Report 79-02 (1979).

$$\sigma_{tot}(E_{c.m.}) = \int d\Omega \left(\frac{d\sigma}{d\Omega} \right)^{elem}_{c.m.}$$

$$= 4\pi\lambdabar^2 A_0(E_{c.m.})$$

Optimal Fermi-averaging (OFA) procedure

T. Harada and Y.Hirabayashi, NPA744 (2004) 323.

- ``Optimal'' cross section for K-p -> K+Ξ⁻ reaction

$$\left(\frac{d\sigma}{d\Omega}\right)^{\rm opt}_{\theta_{\rm lab}} \equiv \beta |\overline{f}_{K^- p \to K^+ \Xi^-}|^2$$

$$= \frac{p_{K^+} E_{K^+}}{(2\pi)^2 v_{K^-}} \left| t^{\rm opt}_{\bar{K}N, K\Xi}(p_{K^-}; \omega, \boldsymbol{q}) \right|^2$$

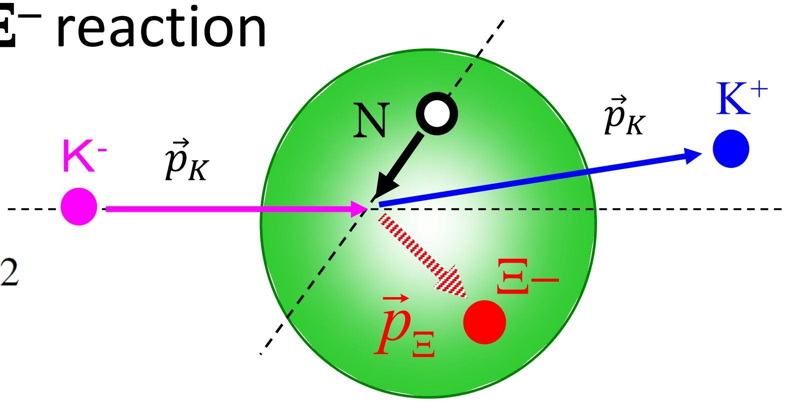

- Optimal Fermi-averaged KN -> KΞ *t*-matrix

$$\cos\theta_N = \hat{\boldsymbol{p}}_{\bar{K}} \cdot \hat{\boldsymbol{p}}_N$$

$$t^{\rm opt}_{\bar{K}N, K\Xi}(p_{\bar{K}}; \omega, \boldsymbol{q})$$

Elementary *t*-matrix

$$= \left. \frac{\int_0^\pi \sin\theta_N d\theta_N \int_0^\infty dp_N p_N^2 \rho(p_N) t_{\bar{K}N, K\Xi}(E_2; \boldsymbol{p}_{\bar{K}}, \boldsymbol{p}_N)}{\int_0^\pi \sin\theta_N d\theta_N \int_0^\infty dp_N p_N^2 \rho(p_N)} \right|_{\boldsymbol{p}_N = \boldsymbol{p}_N^*}$$

momentum dist.

- On-energy-shell equation for a struck proton momentum: $\boldsymbol{p}_N^*$

$$\sqrt{(\boldsymbol{p}_N^* + \boldsymbol{q})^2 + m_\Xi^2} - \sqrt{(\boldsymbol{p}_N^*)^2 + m_N^2} = \omega$$

including the binding effects.

Optimal momentum approximation:
S. A. Gurvitz, PRC33 (1986) 422.

$$\tau = t_a + t_a G_a h G_a t_a + t_a G_a h (G_a + G_a t_a G_a) h G_a t_a + \cdots$$

$h = G_a^{-1} - G^{-1}$ vanishes

``Optimal'' cross section for the $K^{-}p \rightarrow K^{+}\Xi^{-}$ reaction

$$(d\sigma/d\Omega)^{\mathrm{opt}} \qquad \left(\frac{d\sigma}{d\Omega}\right)^{\mathrm{opt}}_{\mathrm{lab}} \equiv \beta|\overline{f}_{K^{-}p\rightarrow K^{+}\Xi^{-}}|^{2}$$

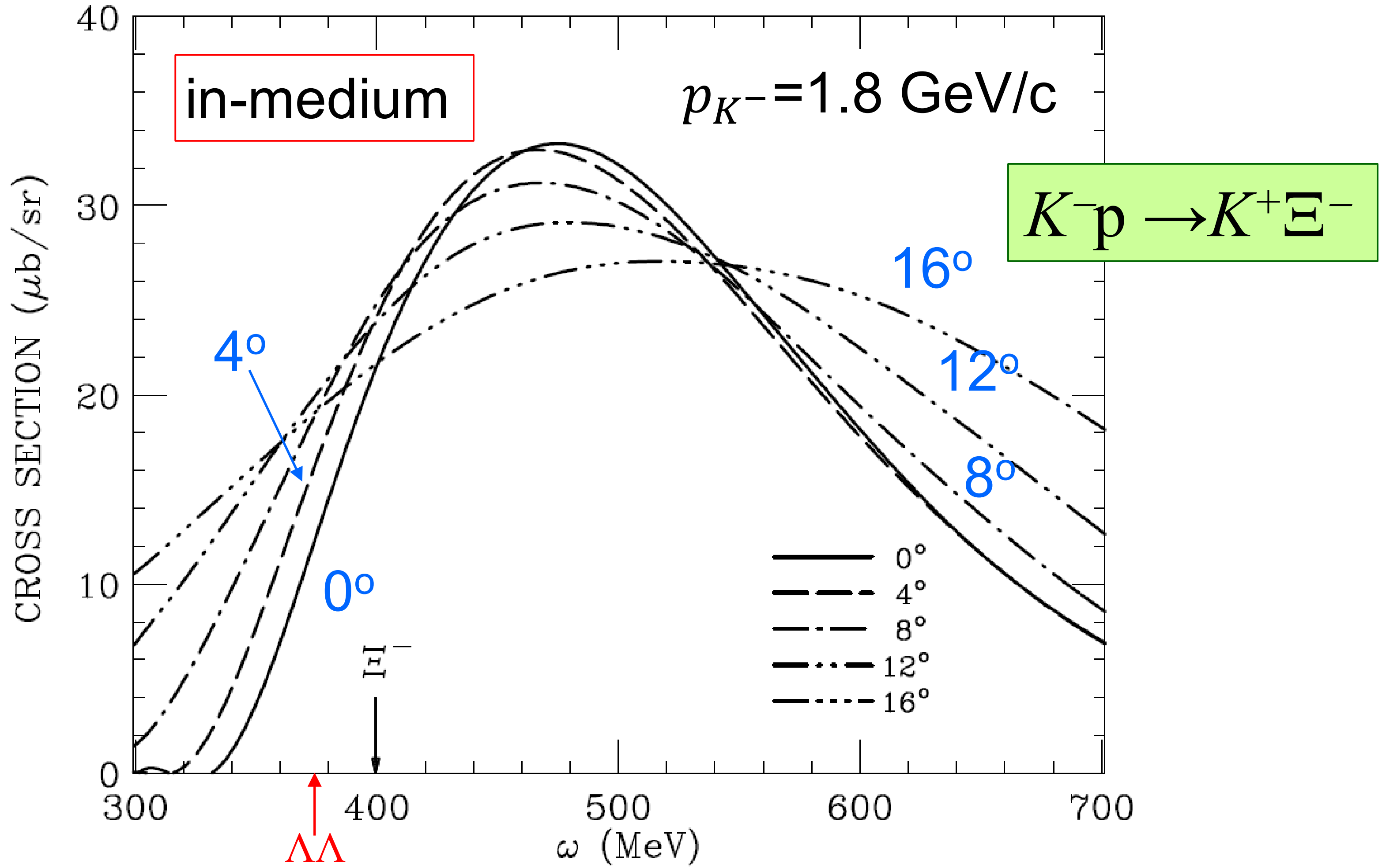

✓ Strong energy and angular dependencies of the cross sections.

Energy dependence of *in-medium* $K^{-}p \rightarrow K^{+}\Xi^{-}$ cross sections

$(d\sigma/d\Omega)^{\mathrm{opt}}$ p_{K^-}=1.8 GeV/c $\beta(d\sigma/d\Omega)^{\mathrm{av}}$

Optimal Fermi averaging (OFA)

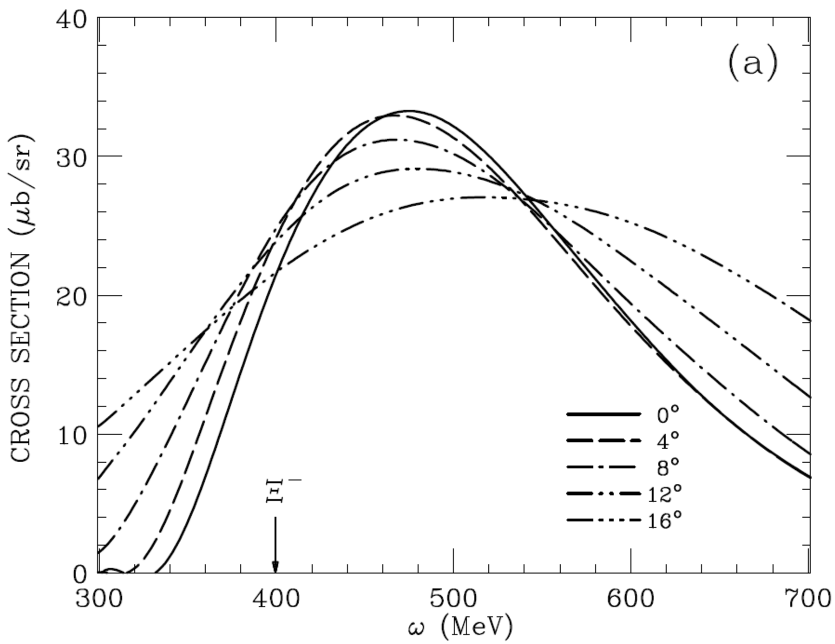

$$\left(\frac{d\sigma}{d\Omega}\right)^{\mathrm{opt}}_{\mathrm{lab}} \equiv \beta|\overline{f}_{K^-p\rightarrow K^+\Xi^-}|^2$$

Ordinary Fermi average in DWIA

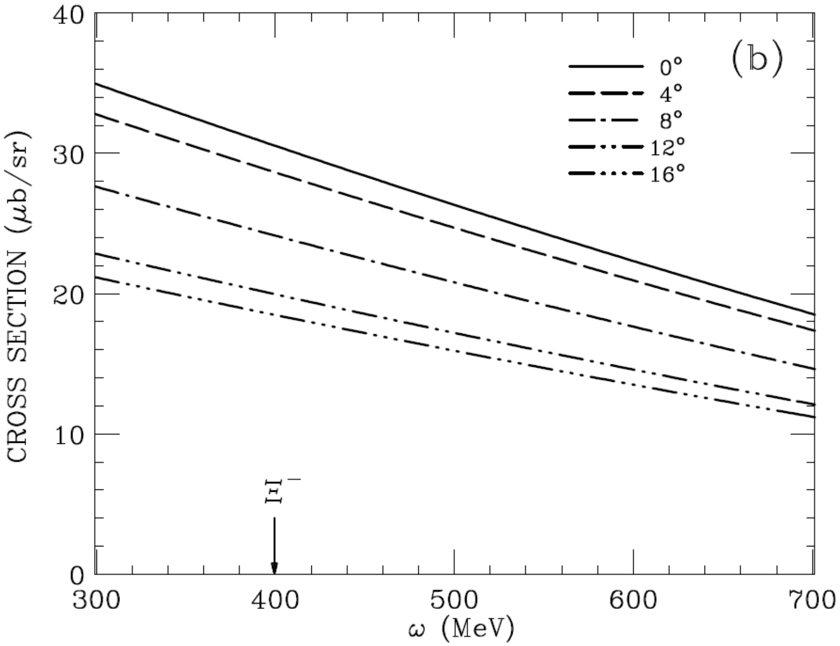

$$\left(\frac{d\sigma}{d\Omega}\right)^{\mathrm{av}}_{\theta_{\mathrm{lab}}} = \int d\boldsymbol{p}_N \rho(p_N)\left(\frac{d\sigma}{d\Omega}\right)^{\mathrm{elem}}$$

Const.

- ✓ The behavior of OFA is very different from that of the ordinary Fermi-averaging.

Application of Optimal Fermi-averaging (OFA) procedure (1)

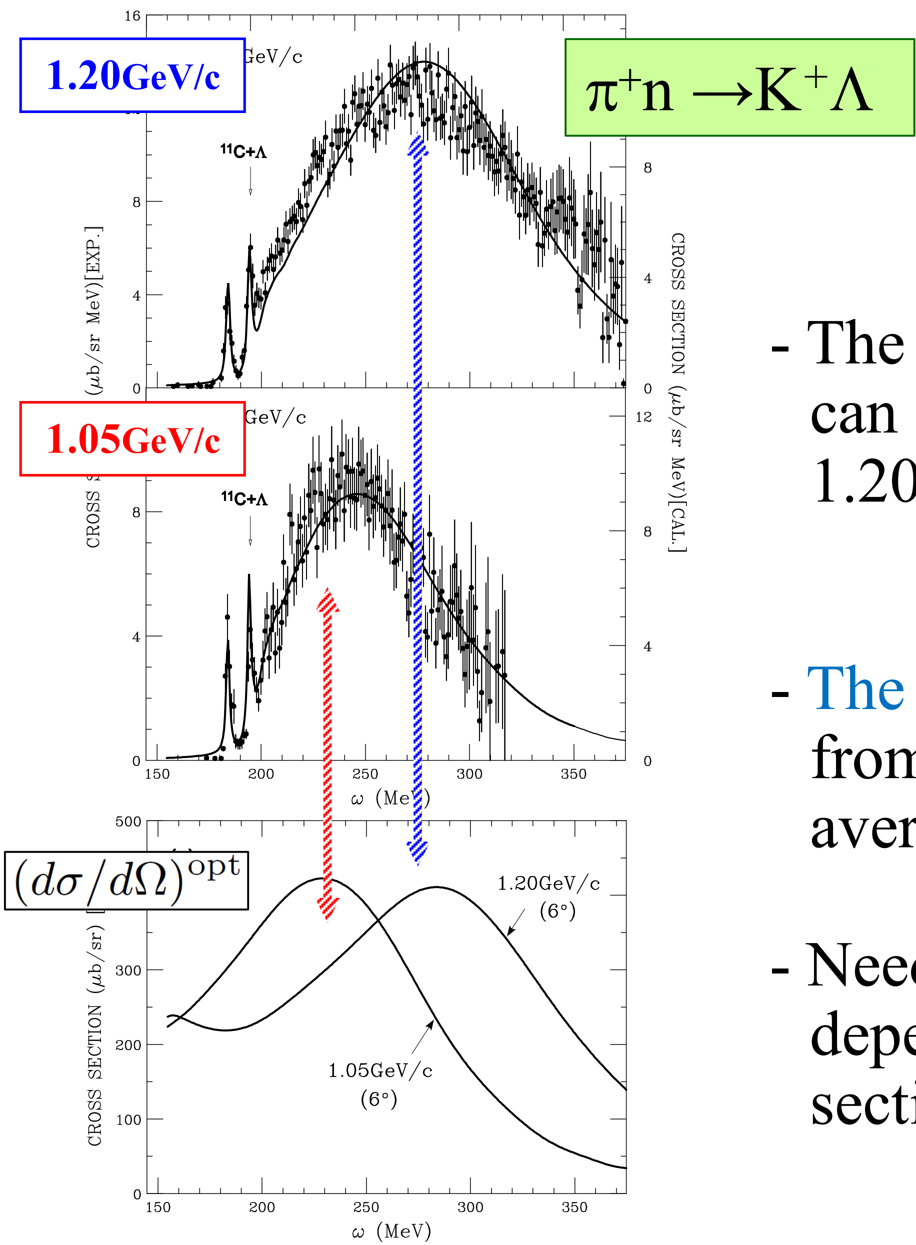

Λ production

^{12}C(π^+, K^+) reactions

- The calculated spectra in the QF region can explain the experimental data at 1.20 and 1.05GeV/c.

This makes the width look narrow.

- The ω energy-dependence originates from the nature of the "optimal Fermi-averaging" t-matrix.

- Need careful consideration for energy-dependent of the elementary cross section.

Application of Optimal Fermi-averaging (OFA) procedure (2)

"$\pi^- p \to K^+ \Sigma^-$ reactions" on the nucleus (^{28}Si, ^{209}Bi, ^{6}Li)

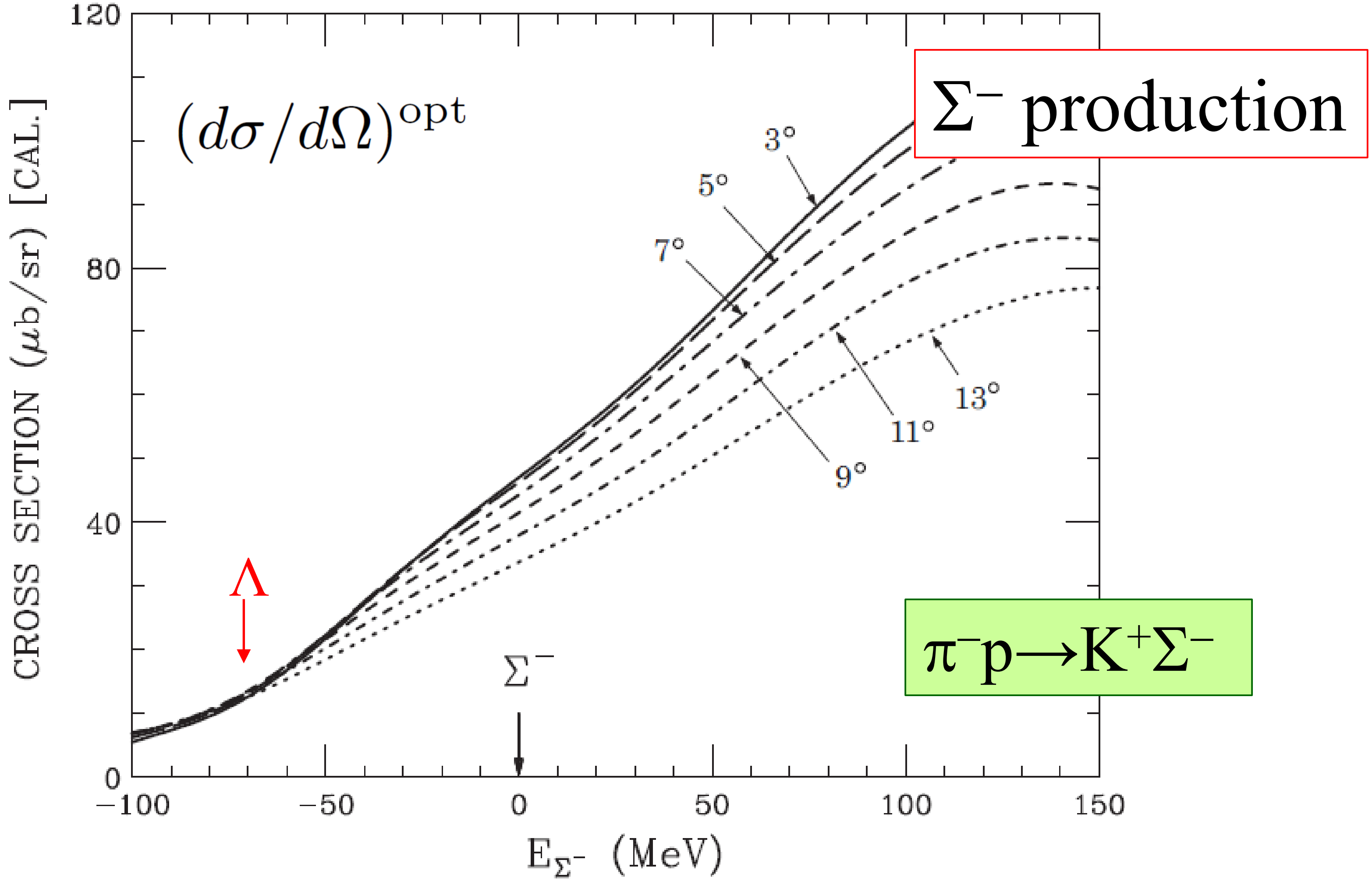

✓ There exists a strong angular and energy dependence in the OFA amplitudes.

Application of Optimal Fermi-averaging (OFA) procedure (3)

$^{28}Si(\pi^-,K^+)$ reaction at 1.2GeV/c

Σ^-

Normalization factor

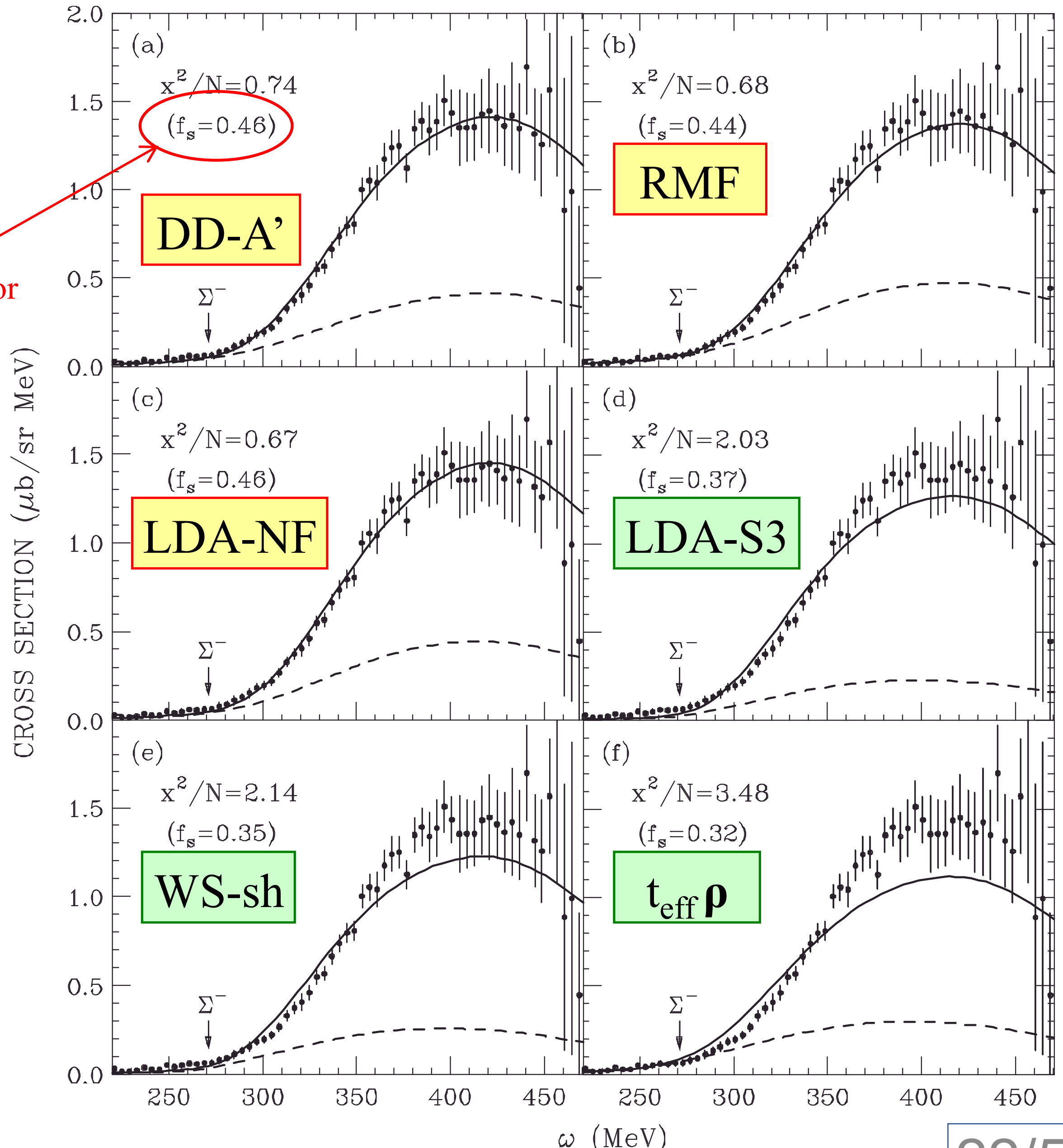

- Calculated spectra with OFA can explain the data of the (π^-, K^+) spectra, by using the Σ-nucleus potentials for fits to the Σ^- atomic X-ray data.

T. Harada, Y. Hirabayashi, NPA759 (2005) 143

2.3
Analysis of Ξ^- QF spectra of the $^9Be(K^-, K^+)$ reaction at BNL-E906

Quasifree Ξ^- production in the ^{9}Be(K$^-$,K$^+$) reaction

T. Tamagawa, Ph.D. thesis, Univ. of Tokyo, 2000 (unpublished).

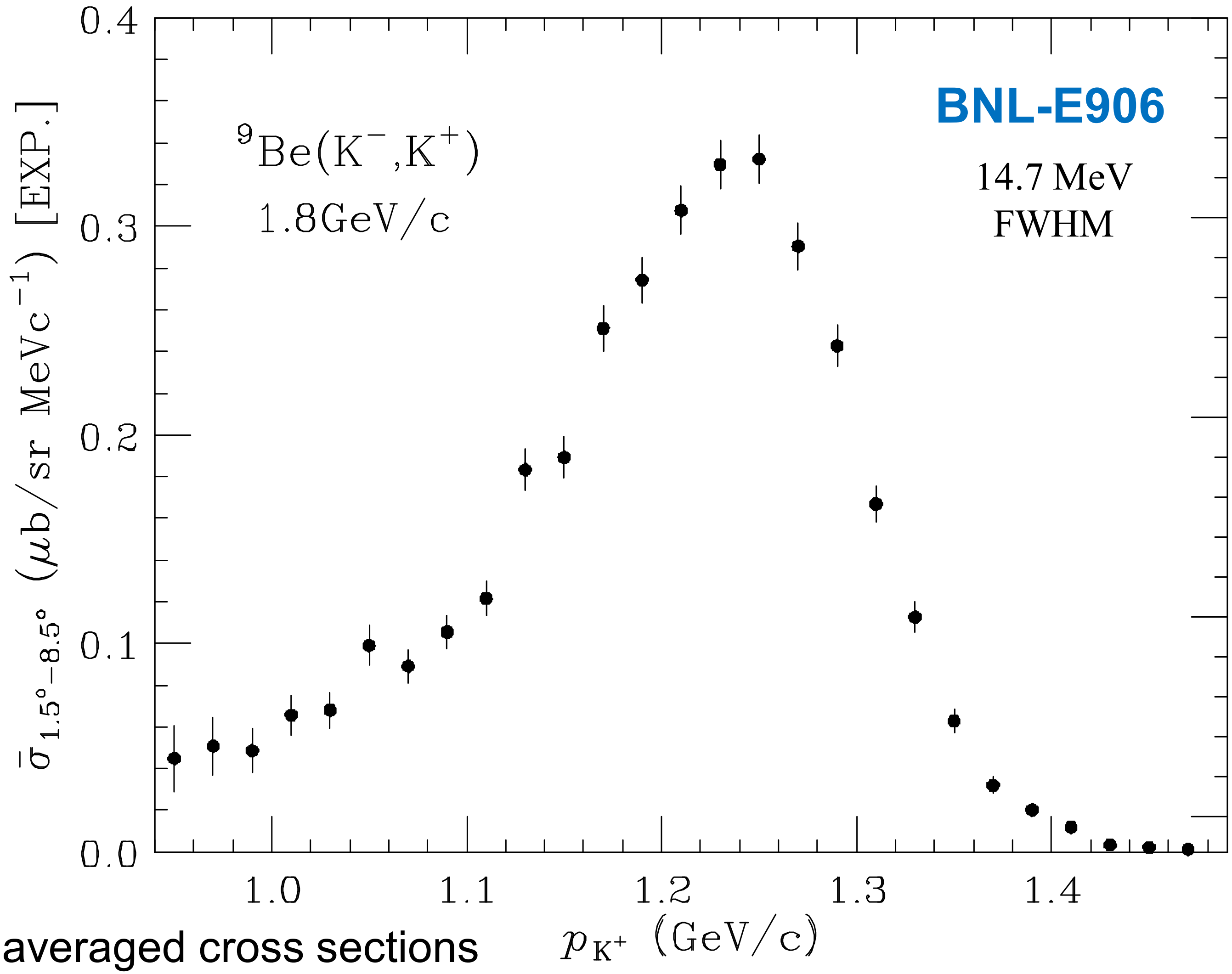

Angular averaged cross sections

$$\bar{\sigma}_{1.5^\circ\text{-}8.5^\circ} \equiv \int_{\theta_{\rm lab}=1.5^\circ}^{\theta_{\rm lab}=8.5^\circ} \left(\frac{d^2\sigma}{dp_{K^+} d\Omega_{K^+}} \right) d\Omega \Big/ \int_{\theta_{\rm lab}=1.5^\circ}^{\theta_{\rm lab}=8.5^\circ} d\Omega.$$

M.Kohno, PRC100 (2019) 024313

SCDW calc.

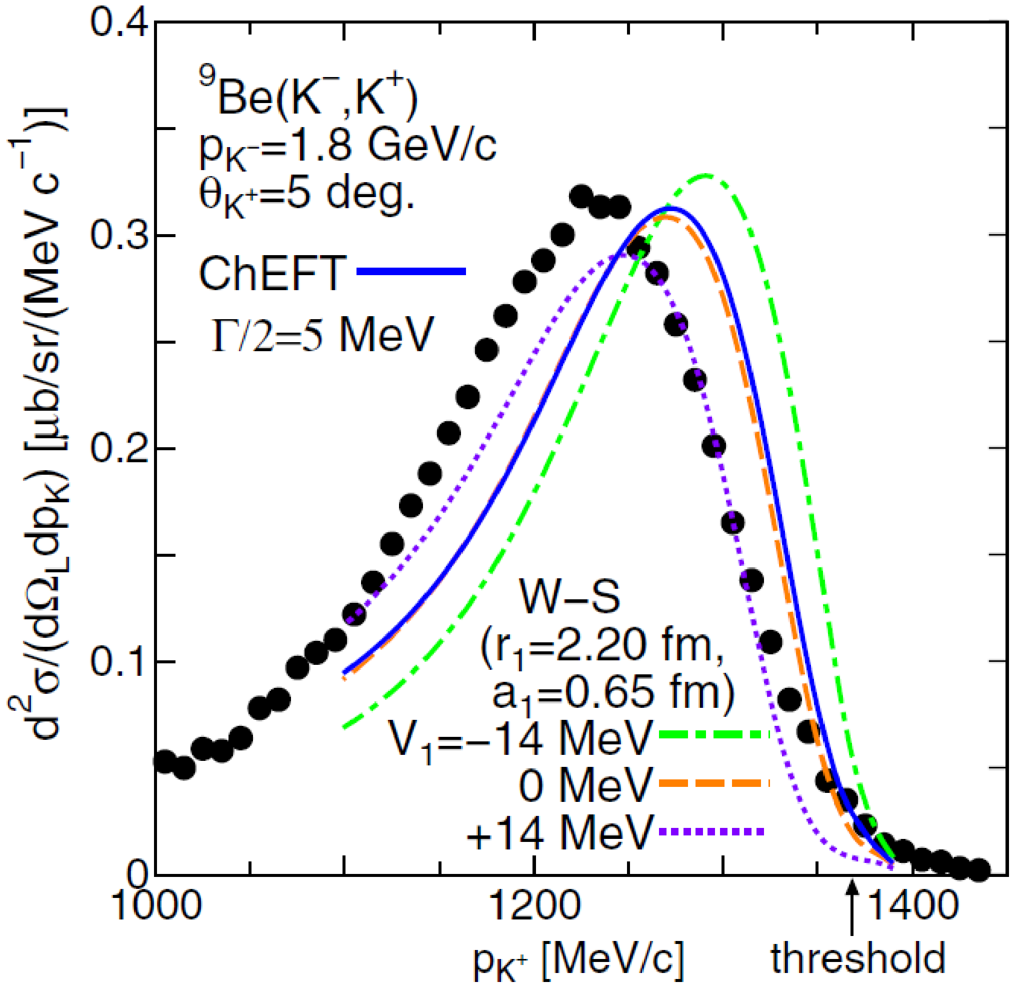

✓ It seems challenging to extract information on the Ξ-nucleus potential because these calculated spectra cannot sufficiently reproduce the data.

Verification of the optimal Fermi-averaged $K^- p \to K^+ \Xi^-$ ampl.

Data: Tamagawa (BNL-E906 collaboration)

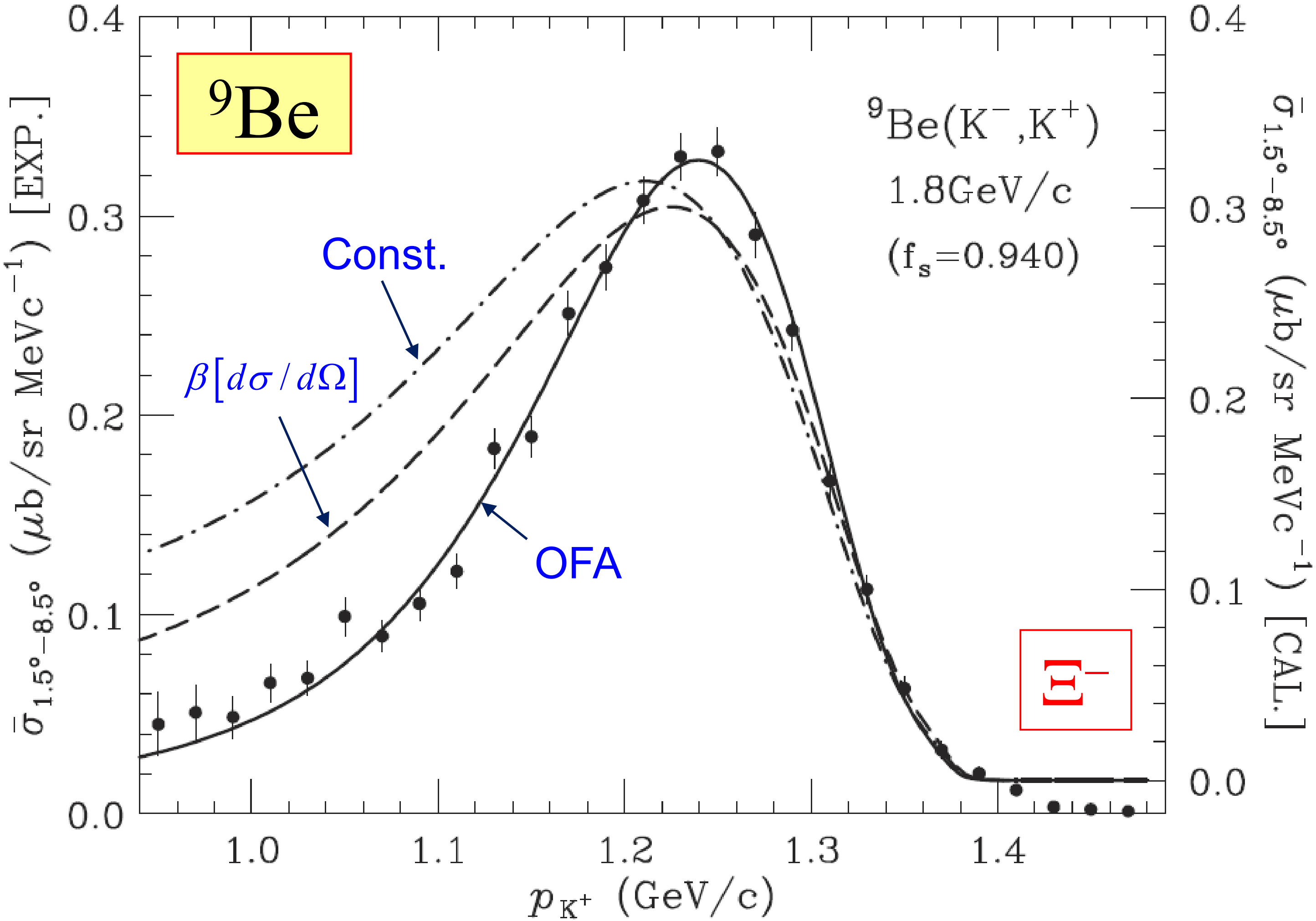

- ✓ This calculated spectrum with OFA improves to reproduce the data of the ^{9}Be(K$^-$, K$^+$) reaction at BNL-E906.

Remarks

- We show the strong energy and angular dependencies of the in-medium $K^{-}p \rightarrow K^{+}\Xi^{-}$ production cross section, which are important to describe the shape and magnitude of the Ξ^{-} production spectrum in the (K^{-}, K^{+}) reaction on the nuclear target.

T. Harada and Y. Hirabayashi, PRC102 (2020) 024618.

- This result may be a basis for the study extracting the properties of the Ξ-nucleus potential from the QF data.
- We expect that an analysis of Ξ^{-} QF spectrum produced via the ^{9}Be(K^{-}, K^{+}) reaction at 1.8 GeV/*c* can extract useful information on the Ξ-nucleus potential for Ξ^{-}-^{8}Li from the data of the BNL-E906 experiment.

2.4
Properties of the Ξ^--^{8}Li potential

Ξ-nucleus potential for Ξ^--^{8}Li

Woods-Saxon pot.

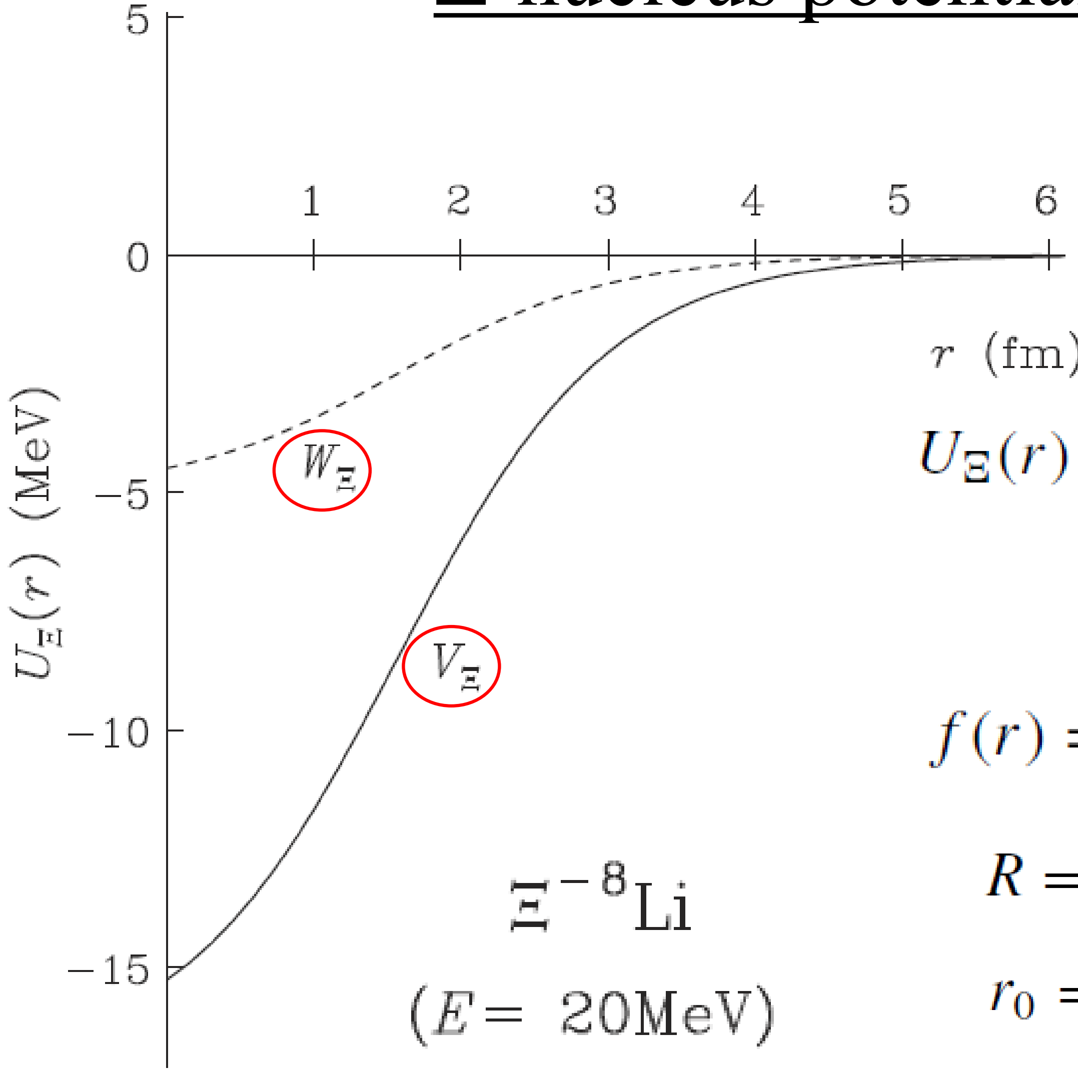

$$U_\Xi(r) = V_\Xi(r) + iW_\Xi(E,r)$$
$$= [V_0^\Xi + iW_0^\Xi g(E)]f(r)$$

fitting parameters

$$f(r) = [1 + \exp\{(r-R)/a\}]^{-1}$$

$$R = r_0 A_{\rm core}^{1/3} = 1.57 \text{ fm}$$

$$r_0 = 0.783 \text{ fm} \quad a = 0.722 \text{ fm}$$

$$\langle r^2\rangle_V^{1/2} = \left[\int r^2 V_\Xi(r) d\boldsymbol{r} \Big/ \int V_\Xi(r) d\boldsymbol{r}\right]^{1/2} = 2.81 \text{ fm}$$

$$V_{\rm so}^\Xi (1/r)[df(r)/dr]\boldsymbol{\sigma}\cdot\boldsymbol{L}$$
$$V_{\rm so}^\Xi \simeq \frac{1}{10} V_{\rm so}^N \simeq 2 \text{ MeV}$$

Effects of the real part of the Ξ-nucleus potential

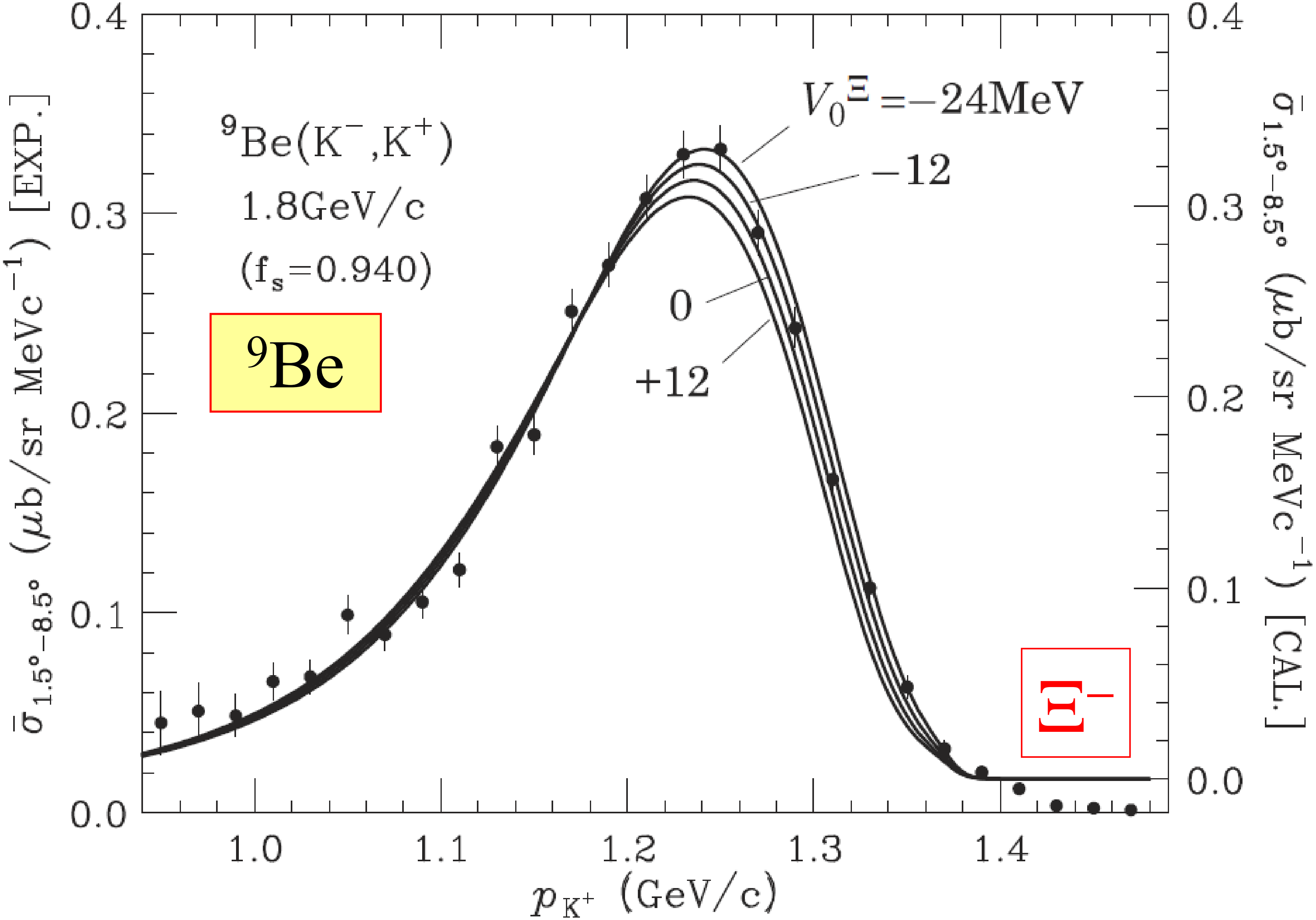

Contour plots of the χ^2-value distribution in $\{V_0, W_0\}$ plane

$$U_\Xi(r) = (V_0 + iW_0)/[1 + \exp\{(r - R)/a\}]$$

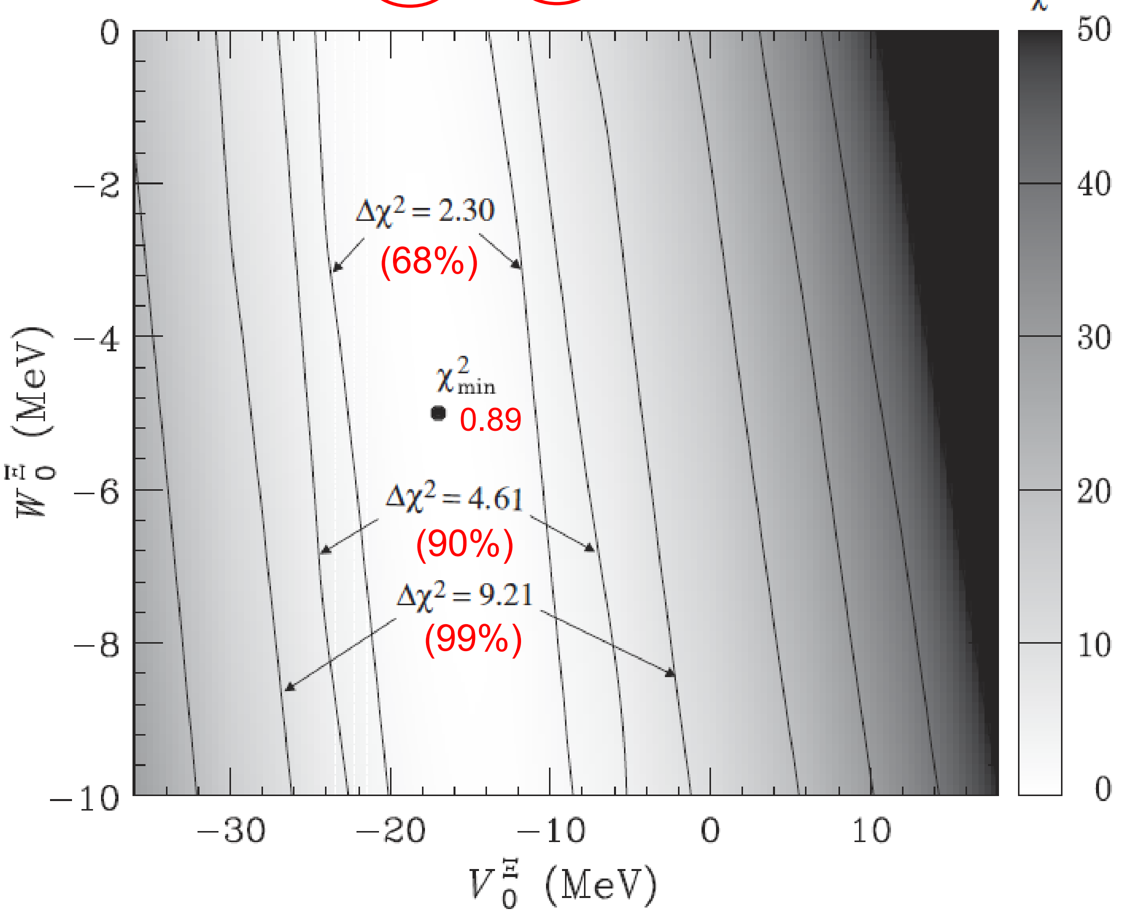

- ✓ The minimum position of χ^2_{min}/N = 15.2/17=0.89, and $\Delta\chi^2$ = 2.30, 4.61, and 9.21 correspond to 68%, 90%, and 99% confidence levels for two parameters, respectively.
- ✓ The value of χ^2 is almost insensitive to W_0.

Ξ-nucleus potential for Ξ^--^{8}Li

Woods-Saxon pot.

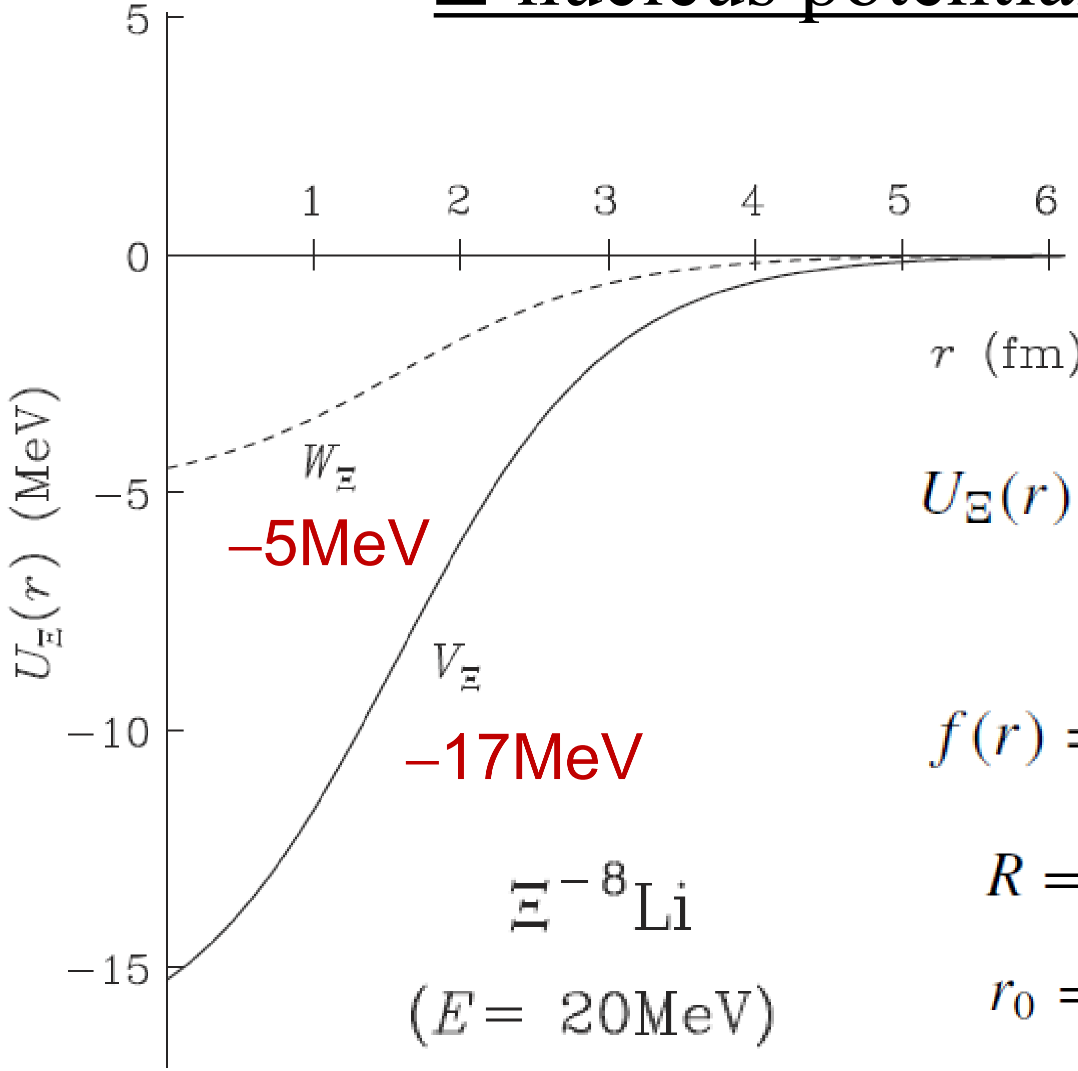

$$U_\Xi(r) = V_\Xi(r) + iW_\Xi(E,r)$$
$$= \left[V_0^\Xi + iW_0^\Xi g(E)\right] f(r)$$

$$f(r) = \left[1 + \exp\{(r-R)/a\}\right]^{-1}$$

$$R = r_0 A_{\rm core}^{1/3} = 1.57 \text{ fm}$$

$$r_0 = 0.783 \text{ fm} \quad a = 0.722 \text{ fm}$$

$$\langle r^2 \rangle_V^{1/2} = \left[\int r^2 V_\Xi(r) d\boldsymbol{r} \Big/ \int V_\Xi(r) d\boldsymbol{r}\right]^{1/2} = 2.81 \text{ fm}$$

$$V_{\rm so}^\Xi (1/r)[df(r)/dr]\boldsymbol{\sigma}\cdot\boldsymbol{L}$$
$$V_{\rm so}^\Xi \simeq \tfrac{1}{10} V_{\rm so}^N \simeq 2 \text{ MeV}$$

Ξ^- QF spectrum by ^{9}Be(K$^-$,K$^+$) reaction at 1.8GeV/c

Data: Tamagawa (BNL-E906 collaboration)

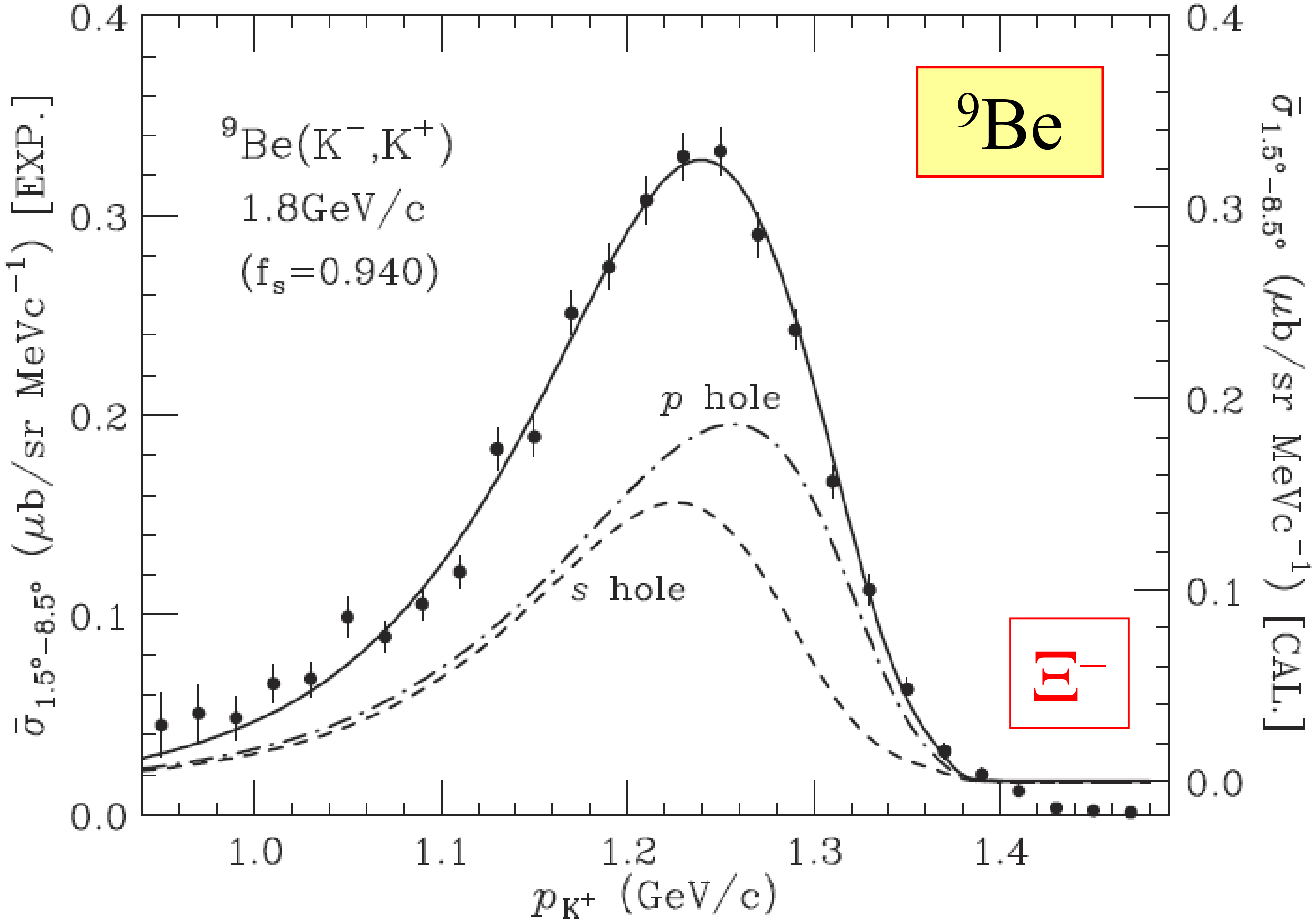

V_0^{Ξ} = –17 MeV, W_0^{Ξ} = –5 MeV

Reduced χ^2 = 15.2/17

✓ The calculated spectrum can explain the data very well.

Validity of the imaginary part of the Ξ-nucleus potential

- The first-order optical potential ($t\rho$)

$$U_{\Xi}^{(1)}(r) = t_{\Xi^- p}\rho_p(r) + t_{\Xi^- n}\rho_n(r)$$

- The imaginary part of $U_{\Xi}^{(1)}$

The optical theorem

$$4\pi \, \mathrm{Im} \, f_{\Xi N}(0) = k_{\Xi}\sigma_{\mathrm{tot}}$$

$$W_{\Xi}^{(1)}(r) = -\langle v_{\Xi^- p}\sigma(\Xi^- p \rightarrow \Xi^0 n, \Lambda\Lambda)\rangle \rho_p(r)/2$$

Gal, Toker, Alexander, Ann. Phys. **137** (1981) 341.

- In-medium cross section

(Pauli correction + C.M. correction + Fermi-averaging)

$$\langle v_{\Xi^- p}\sigma(\Xi^- p \rightarrow \Xi^0 p, \Lambda\Lambda)\rangle \qquad \langle v_{\Xi^- p}\sigma(\Xi^- p \rightarrow \Lambda\Lambda)\rangle$$

- $\Xi^- p$ reaction cross sections

$$v_{\Xi^- p}\sigma = (v_{\Xi^- p}\sigma)_0/(1 + \alpha v)$$

velocity: v parameters: $(v_{\Xi^- p}\sigma)_0, \alpha$

$\Xi^- p$ reaction cross sections in ChiEFT

$\Xi^- p \to \Xi^0 p, \Lambda\Lambda$ reactions

Haidenbauer and Meiner, EPJ. A **55**, 23 (2019).

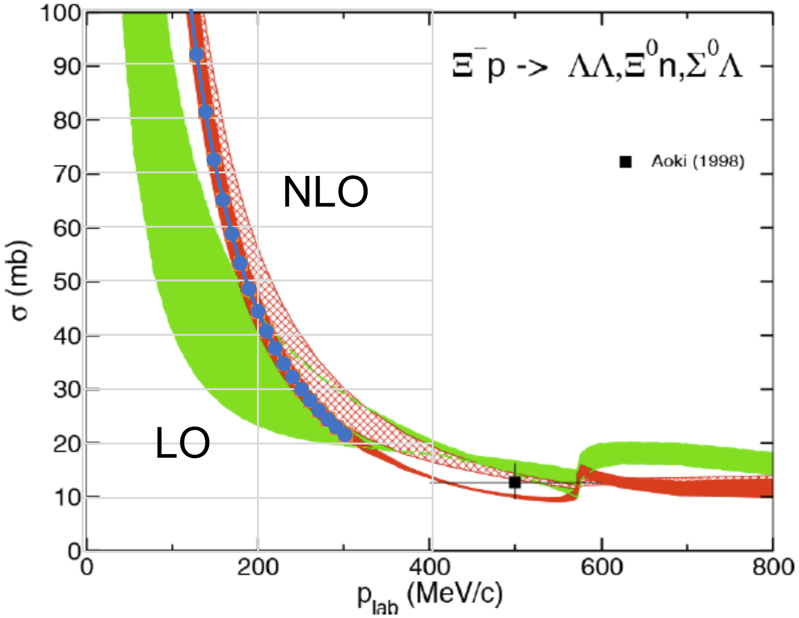

□ $(v_{\Xi^- p}\sigma)_0 = 25\text{mb}, \quad \alpha = 18$

$\langle v_{\Xi^- p}\sigma \rangle = 7.02 \text{ mb}$

$\mathrm{Im} b = \mu \langle v\sigma \rangle / 8\pi = 0.078 \text{ fm}$

$W_0 = -6.2$ MeV

$\Xi^- p \to \Lambda\Lambda$ reactions

Haidenbauer et al, NPA **954**, 273 (2016).

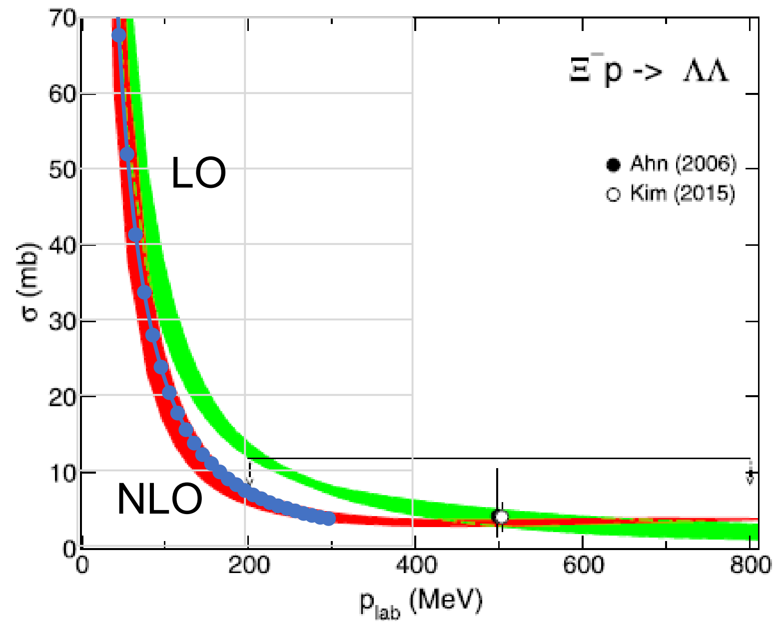

□ $(v_{\Xi^- p}\sigma)_0 = 4.5\text{mb}, \quad \alpha = 20$

$\mathrm{Im} b = 0.018 \text{ fm}$

$W_0 = -1.5$ MeV

Remarks

- We have studied phenomenologically the Ξ^- production spectrum of the ^{9}Be(K^-,K^+) reaction at 1.8 GeV/c within the DWIA using the optimal Fermi-averaged $K^- p \to K^+ \Xi^-$ amplitude.
- The weak attraction in the Ξ-nucleus potential for Ξ^--^{8}Li provides the ability to explain the BNL-E906 data, consistent with analyses for previous experiments:

$$V_0 = -17 \pm 6 \text{ MeV} \quad \text{for } W_0 = -5 \text{ MeV}$$

It is difficult to determine the value of W_0 from the data due to the insufficient resolution of 14.7 MeV FWHM.

T. Harada and Y. Hirabayashi, PRC103 (2021) 024605.

3. Properties of Ξ-nucleus potentials

IBUKI (J-PARC E07)

$$\Xi^- + {}^{14}N \rightarrow {}^{10}_{\Lambda}Be(\#1) + {}^{5}_{\Lambda}He(\#2),$$

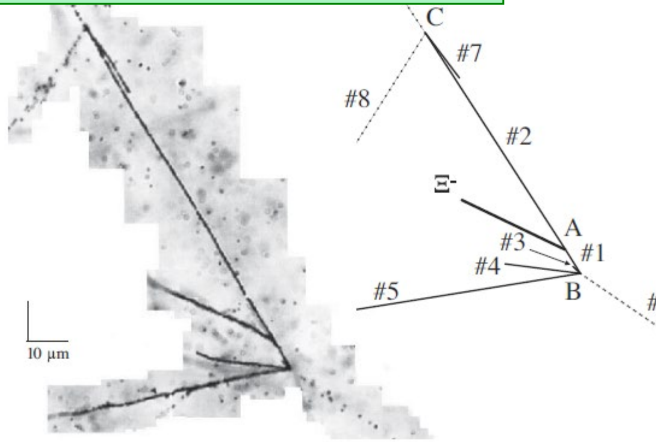

B_{Ξ^-} = 1.27±0.21 MeV

Hayakawa, et al., PRL**126**, 062501 (2021).

Event	Target	Decay mode		B_{Ξ^-} [MeV]
KISO [9,10]	^{14}N	$^{10}_{\Lambda}Be$	$^{5}_{\Lambda}He$	3.87 ± 0.21
	^{14}N	$^{10}_{\Lambda}Be^*$	$^{5}_{\Lambda}He$	1.03 ± 0.18
IBUKI (present data)	^{14}N	$^{10}_{\Lambda}Be$	$^{5}_{\Lambda}He$	1.27 ± 0.21

B_{Ξ} (2p) = 1.03 ±0.18 MeV (KISO) and 1.27 ±0.21 MeV (IBUKI), which suggested to form a Coulomb-assisted nuclear 2p bound state for Ξ^-.

IRRAWADDY (J-PARC E07)

$$\Xi^- + {}^{14}N \rightarrow {}^{5}_{\Lambda}He\ (\#1) + {}^{5}_{\Lambda}He\ (\#2) + {}^{4}He\ (\#3) + n$$

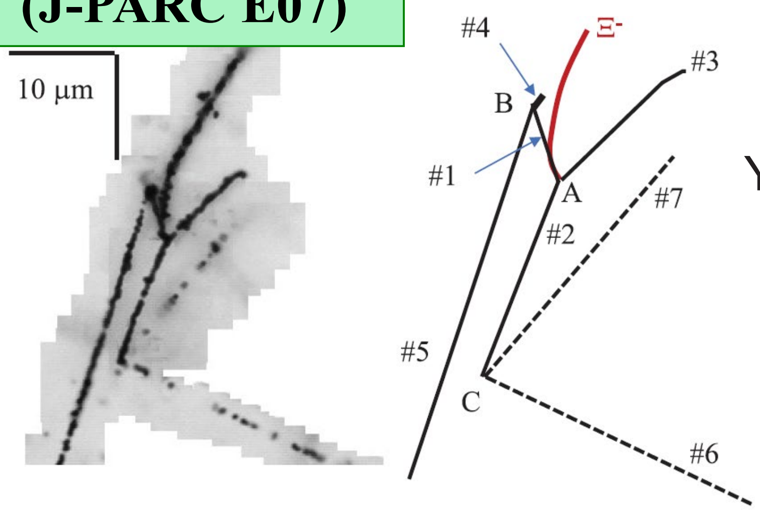

B_{Ξ^-} = 6.27±0.27 MeV

Yoshimoto, et al., PTEP **2021**, 073D02(2021).

New events give the first indication of the nuclear 1s state of $\Xi^{-14}N$, and suggest that the ΞN-$\Lambda\Lambda$ coupling is weak.

Recent observations of Ξ^- hypernuclei from emulsion compared with theoretical predictions

$\Xi^- + {}^{14}N$

M. Yoshimoto, Prog. Theor. Exp. Phys. **2021**, 073D02.

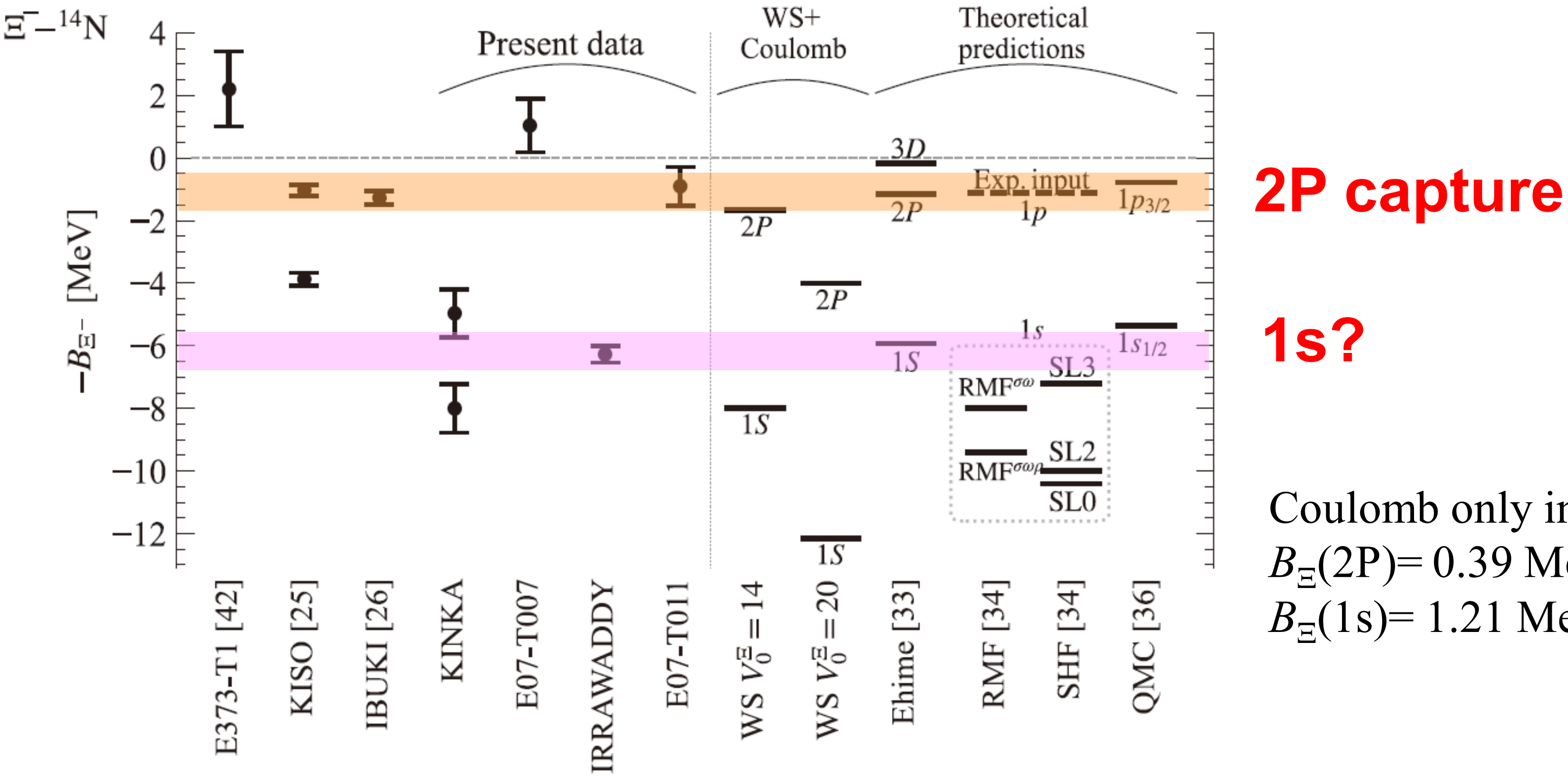

Coulomb only in $\Xi^- {}^{14}N$:
B_Ξ(2P)= 0.39 MeV
B_Ξ(1s)= 1.21 MeV

✓ Ξ^- capture from the 2P state: B_Ξ (2P) = 1.03 MeV(KISO)-1.27 MeV (IBUKI)
- The Ξ-nucleus potential is attractive in the real part.
- The 2P capture rate (4%) obtained from cascade cal.
  → ΞN-ΛΛ coupling is weak (consistent with HAL-QCD).

Ξ^- absorption cascade process in Ξ^--^{14}N atom

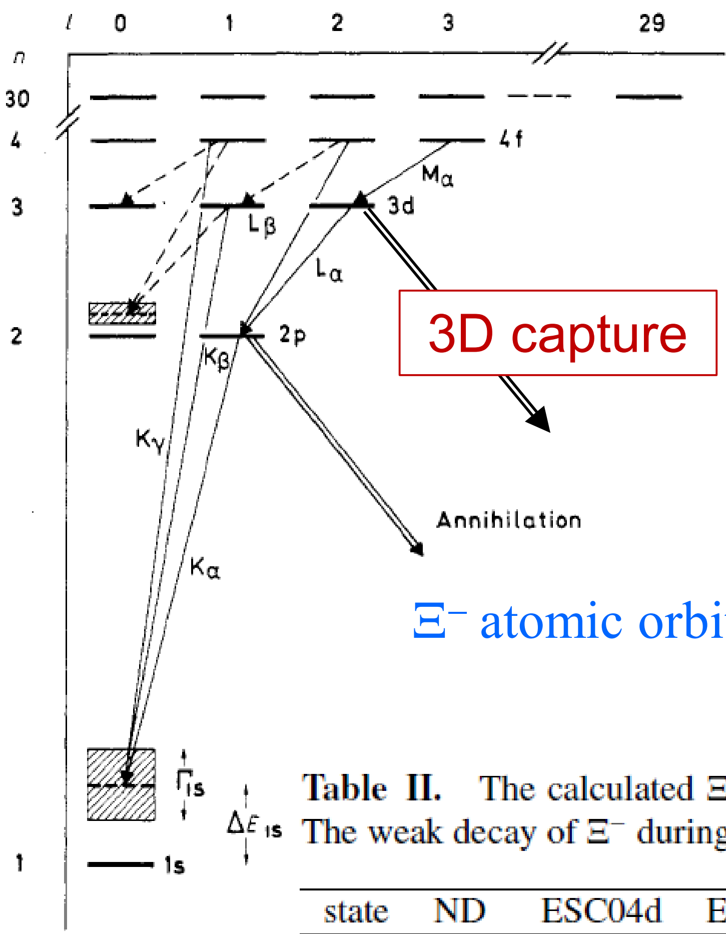

D. Zhu, et al., PRL 67 (1991) 2268.

TABLE I. Calculated Ξ^- capture probabilities (in %) from s, p, d, and f atomic orbits,[a] for various choices of Ξ^--nucleus real and imaginary potential-well depths[b] V_0 and W_0.

Target	V_0 (MeV)	W_0 (MeV)	s	p	d	f
^{6}Li	23.7	6.4	0.04	18.6	80.6	⋯
	23.7	3.2	0.04	30.3	68.9	⋯
	0	3.2	0.07	35.7	63.4	⋯
^{14}N	28.6	7.7	0.00	0.2	54.1	45.6
	28.6	3.9	0.03	0.4	69.9	29.6
	0	3.9	0.03	1.3	75.7	22.9

Ξ^- atomic orbits $(nl)_\Xi$ with $l_\Xi = l_p$ due to $\Xi^- p \to \Lambda\Lambda$ $^1S_0$ channel.

T. Koike, JPS Conf. Proc. **17**, 033011 (2017).

Table II. The calculated Ξ^- nuclear absorption probability (in % per stopped Ξ^-) from each atomic state. The weak decay of Ξ^- during the cascade is 8.2% for any potentials.

state	ND	ESC04d	ESC08c	ESC08c-A	state	ND	ESC04d	ESC08c	ESC08c-A
1s	0.02	3×10^{-4}	1×10^{-4}	0.01	total s	0.07	0.04	0.06	0.06
2p	3.9	0.25	3.8	2.4	total p	5.7	0.88	5.7	4.0
3d	35.7	23.5	34.7	34.9	total d	67.1	47.9	65.3	65.3
4f	7.8	19.0	8.6	9.4	total f	18.9	42.9	20.8	22.5
5g	0.01	0.03	0.01	0.01	total g	0.03	0.10	0.04	0.04

Ξ^--^{14}N absorption: *3D* ~ 35%, *2P* ~ 4%, *1S* < 0.1%

ΛΛ and ΞN interactions from lattice QCD near the physical point

K. Sasaki et al.(HAL QCD Collaboration), NP998 (2020) 121737.

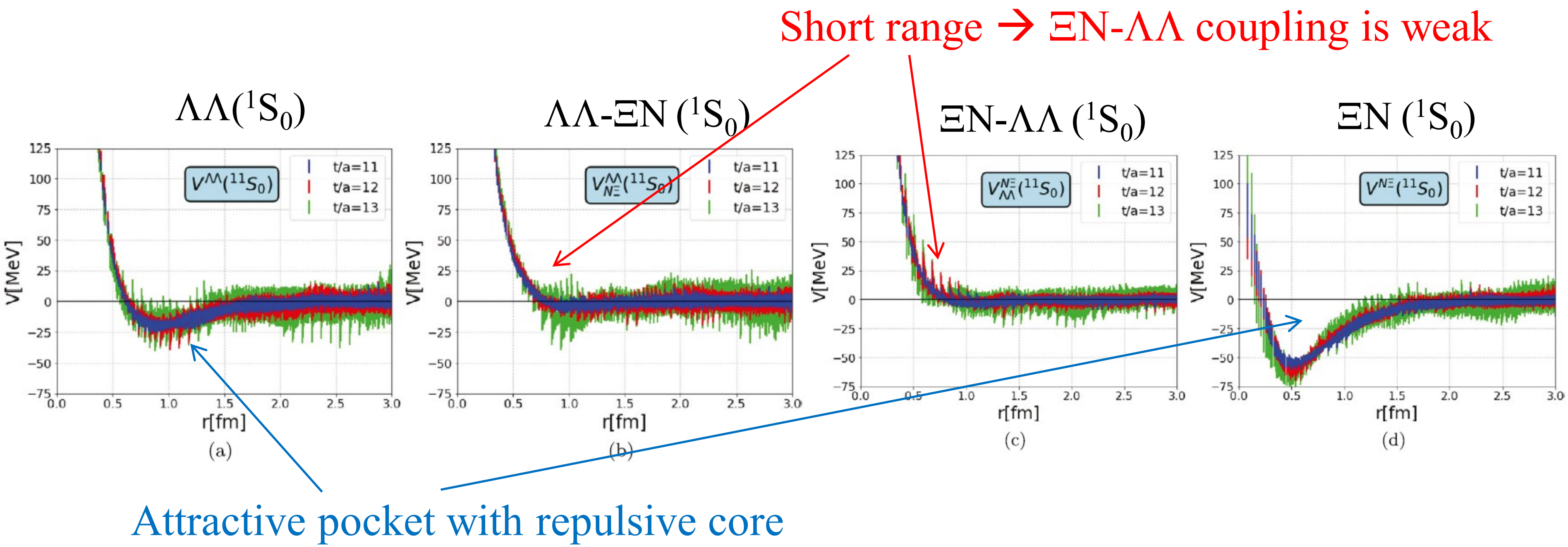

which implies that the leading-order truncation of the derivative expansion is reasonable. The diagonal potentials, $V^{\Lambda\Lambda}$ and $V^{N\Xi}$ in Fig. 1 (a, d), have attractive pocket with a long-range tail together with a short-range repulsive core. From the meson exchange picture, the one-pion exchange is allowed only in $N\Xi$-$N\Xi$ channel. One interesting feature is that the overall attraction in $V^{N\Xi}$ is substantially larger than that in $V^{\Lambda\Lambda}$. The off-diagonal potentials shown in Fig. 1 (b, c) are found to be non-zero only at short distance, which suggests that the $\Lambda\Lambda$-$N\Xi$ coupling is weak at low energies.

Remarks

- KEK-E224 and BNL-E885: Fukuda et al., (1998)
  $-V_0^{\Xi}$ = 14 MeV, < 20 MeV Khaustov et al. (2000)
- BNL-E906:
  $-V_0^{\Xi}$ = 17±6 MeV Harada-Hirabayashi (2021)
- Density dependence of $V_0^{\Xi}(\rho_0)$:
  $-V_0^{\Xi}(\rho_0)$ = 21.9±0.7 MeV Friedman-Gal (2021)
- Microscopic calculations + ΞN G-matrix
  Lattice QCD, ChEFT: **$-V_0^{\Xi}$ < 10 MeV**
  Ehime, NHD, NSC08, NSC16, …
- Contributions of ΞN→ΛΛ coupling and ΞNN force
  weak (from HAL-QCD)

Interpretation of Ξ^- binding energies B_Ξ for Ξ^--^{14}N

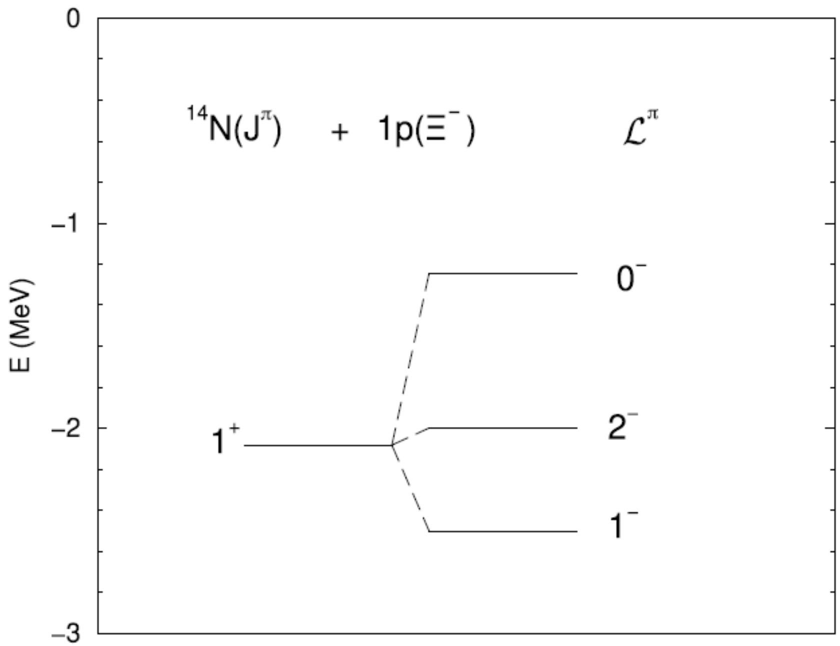

Friedman, Gal, PLB 820 (2021) 136555.

Residual ΞN interaction

$$\mathcal{V}_{\Xi N} = F^{(2)}_{\Xi N} Q_N \cdot Q_\Xi ,$$

$$Q_B = \sqrt{\frac{4\pi}{5}} Y_2(\hat{r}_B)$$

$V_0^\Xi = -21.9 \pm 0.7$ MeV

capture from $1p_{\Xi^-}$ Coulomb-assisted bound states. This involved using just one *common* strength parameter of a density dependent optical potential. Long-range ΞN shell-model correlations were essential in making the ^{14}N events consistent with the ^{12}C events. Earlier attempts to explain these data overlooked this point, therefore reaching quite different conclusions [50–54]. Predicted then are $1s_{\Xi^-}$ bound states with $B^{1s}_{\Xi^-} \sim 10$ MeV in ^{12}C and somewhat larger in ^{14}N, deeper by 4–5 MeV than the $1s_{\Xi^-}$ states claimed by

Ξ^- Binding energies B_{Ξ^-} for twin Λ hypernuclei in emulsion (E176/E373/E07)

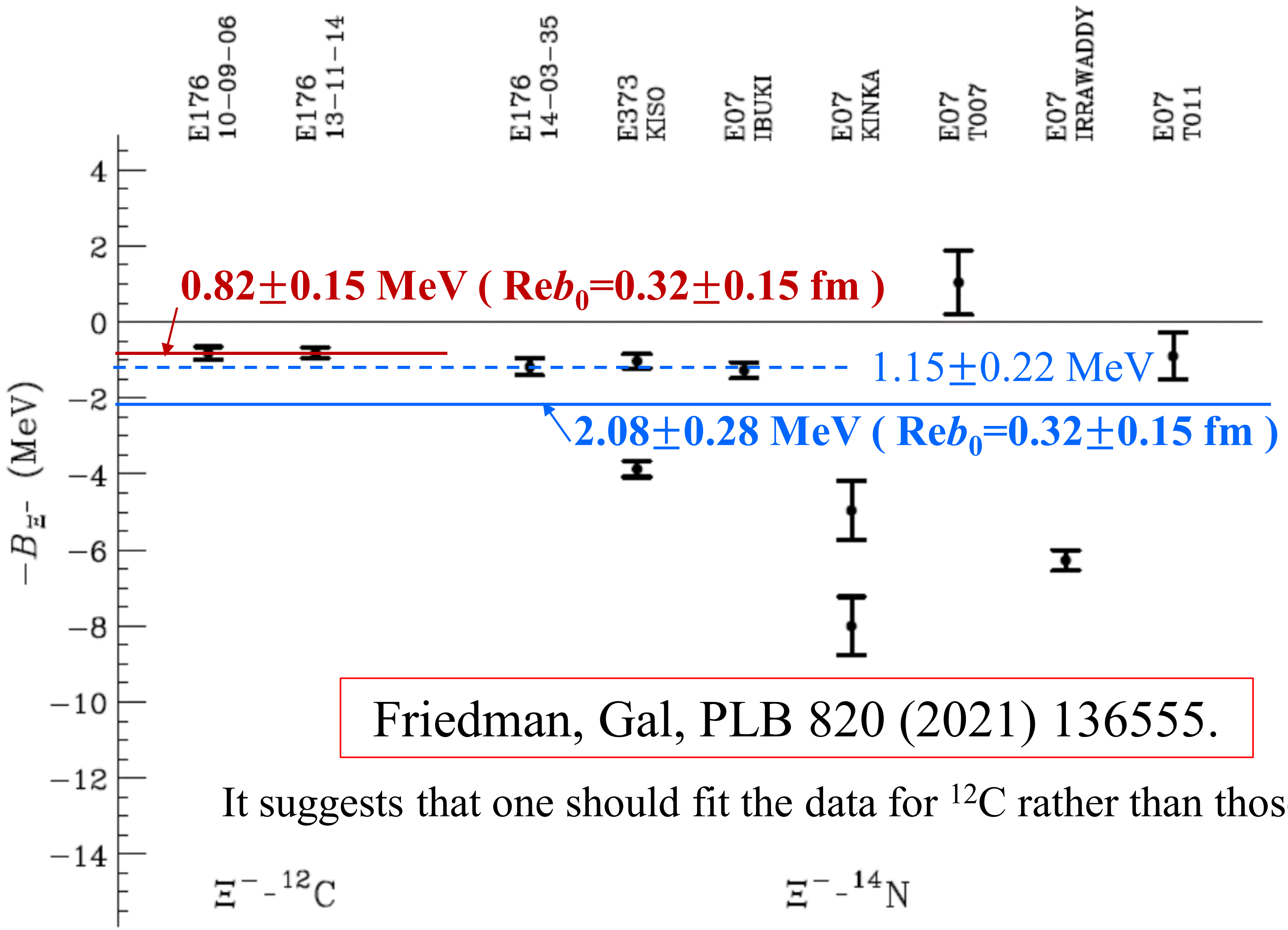

Friedman, Gal, PLB 820 (2021) 136555.

It suggests that one should fit the data for ^{12}C rather than those for ^{14}N.

Ξ^--^{12}C vs. Ξ^--^{14}N

Dependence of V_0^{Ξ} strength in the Ξ-nucleus potentials

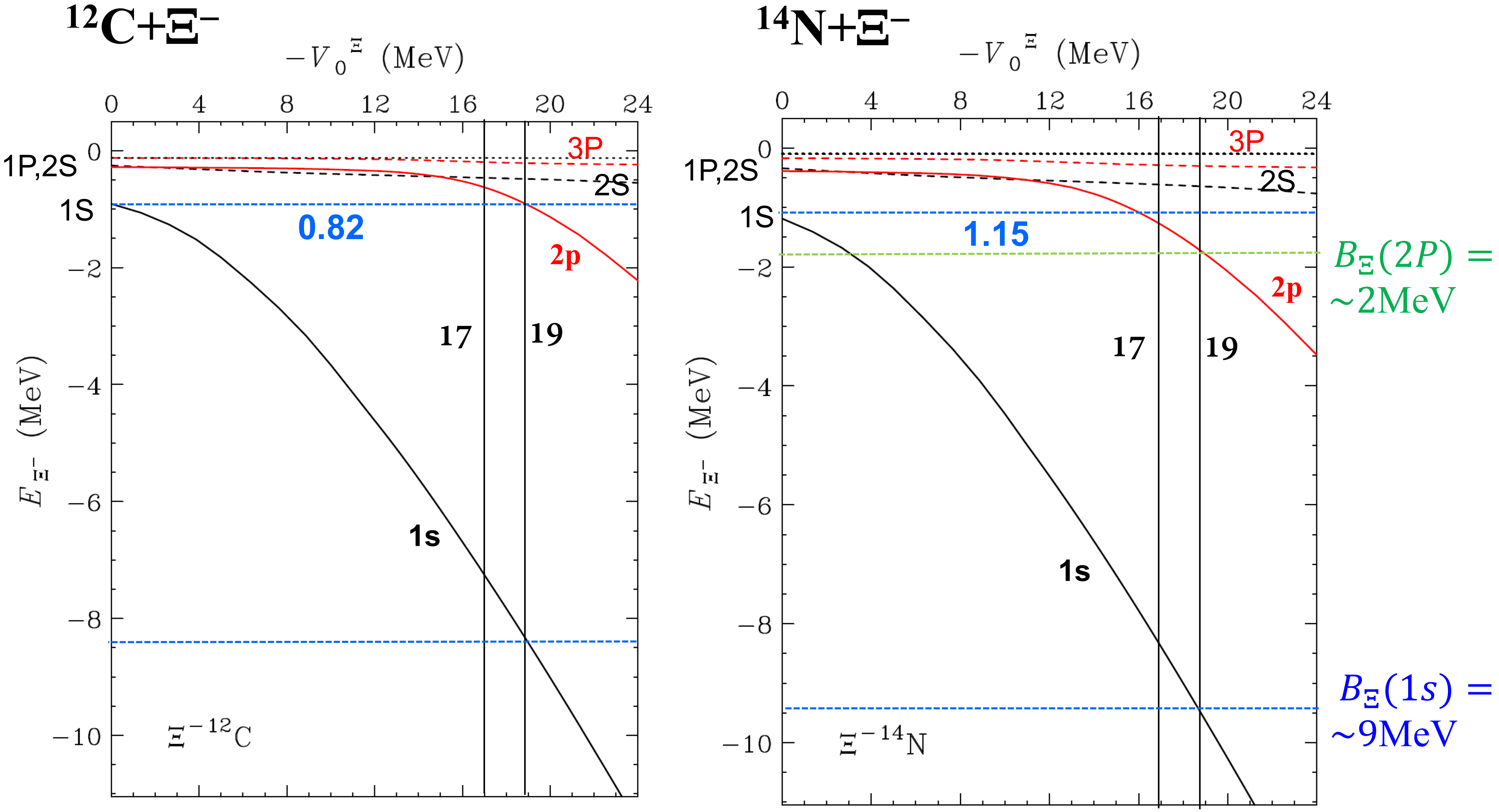

✓ The Ξ-nucleus WS potential for ^{12}C is inconsistent with that for ^{14}N for reproducing the data; $-V_0$ = 17 MeV → 19 MeV, and we confirmed FG.

Ξ^--nucleus optical potential for $^{12}C+\Xi^-$

WS and theoretical potentials by microscopic calculations

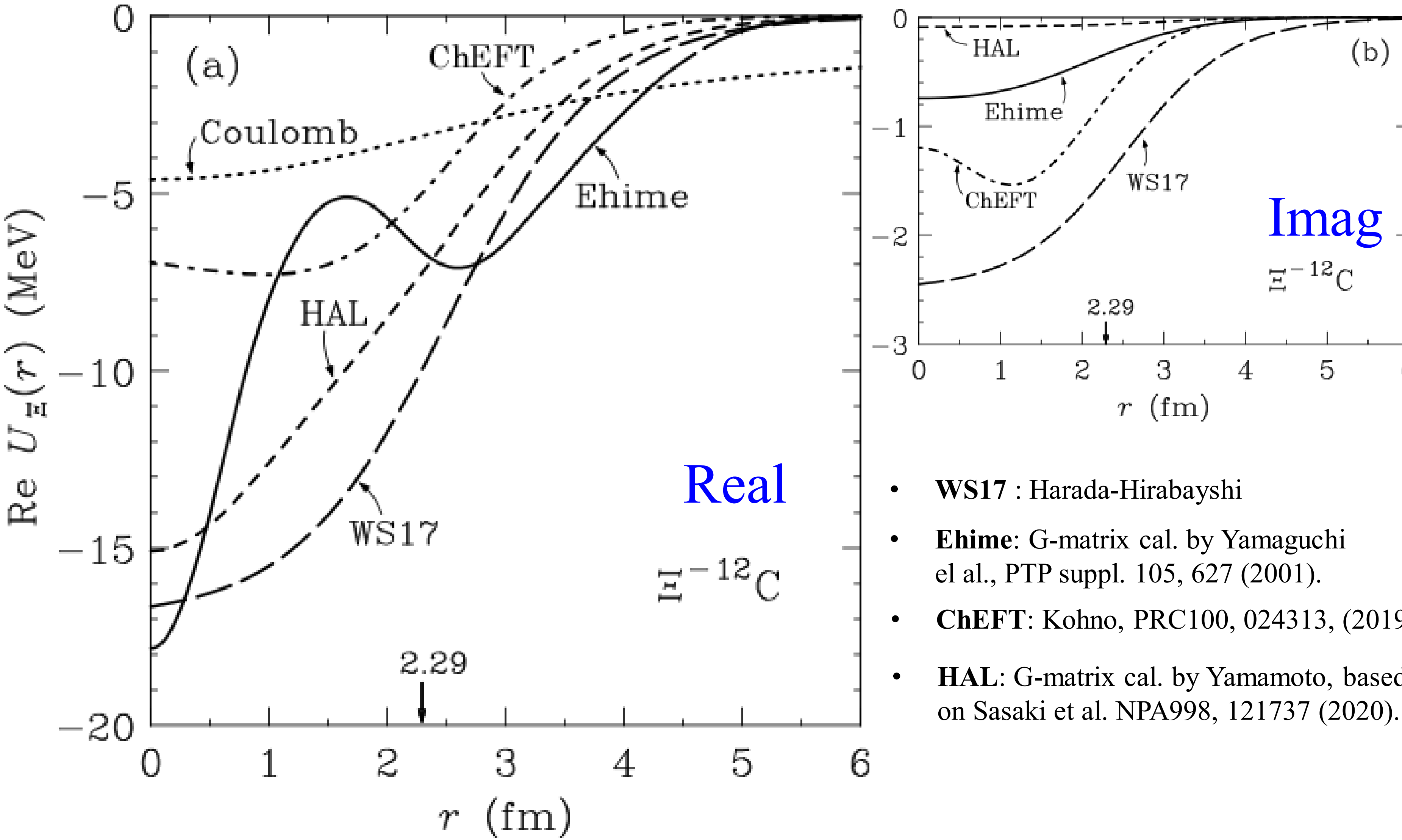

- **WS17** : Harada-Hirabayshi
- **Ehime**: G-matrix cal. by Yamaguchi el al., PTP suppl. 105, 627 (2001).
- **ChEFT**: Kohno, PRC100, 024313, (2019).
- **HAL**: G-matrix cal. by Yamamoto, based on Sasaki et al. NPA998, 121737 (2020).

Ξ-nucleus states in $^{12}C+\Xi^-$

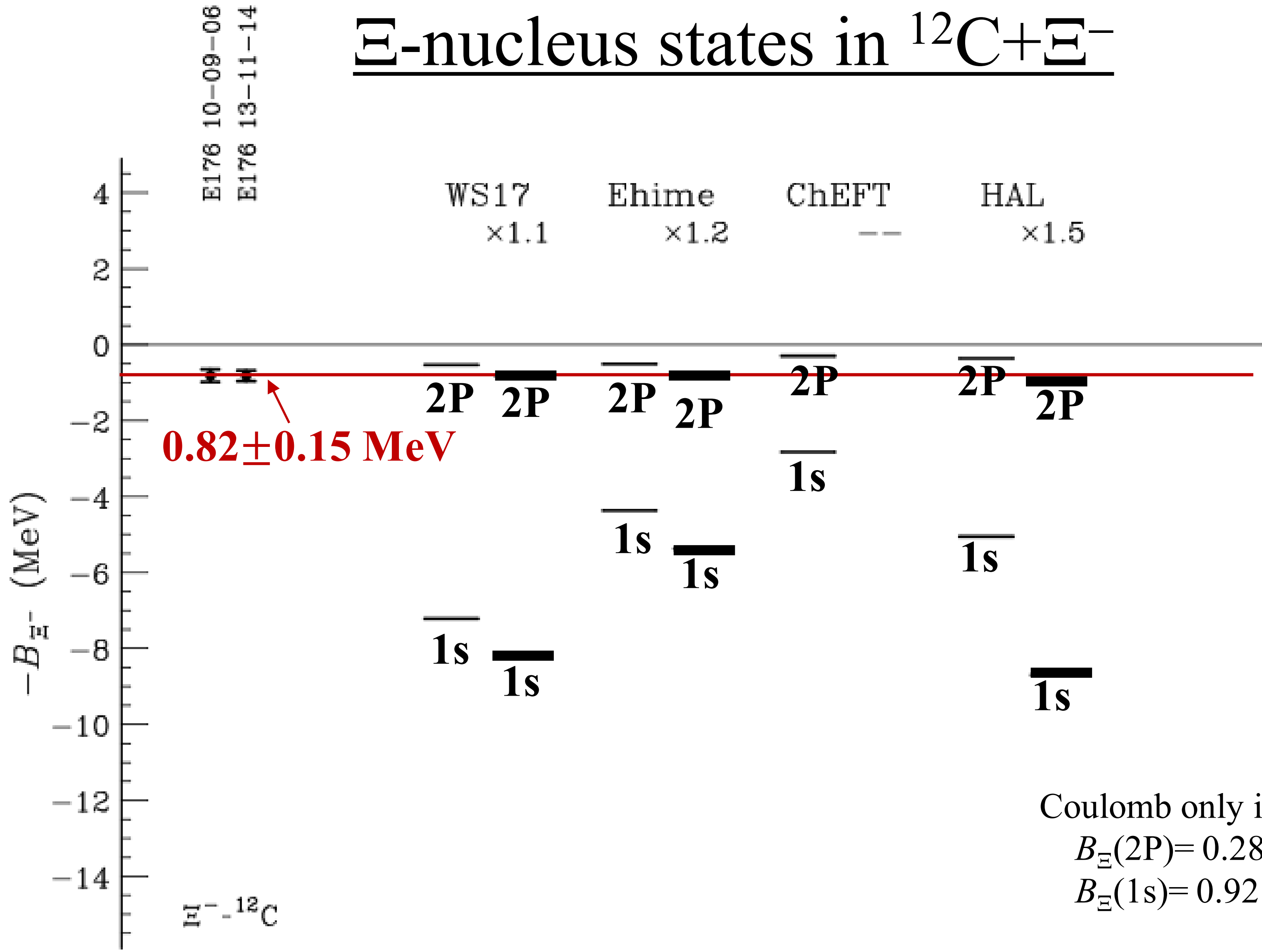

Coulomb only in $\Xi^{-12}C$:
$B_\Xi(2P) = 0.28$ MeV
$B_\Xi(1s) = 0.92$ MeV

✓ If we fit the experimental value of B_Ξ for ^{12}C-Ξ^- 2P state by introducing artificial factors, it suggests that the potential strengths are more attractive.

Ξ^--nucleus optical potential for $^{14}N+\Xi^-$

WS and theoretical potentials by microscopic calculations

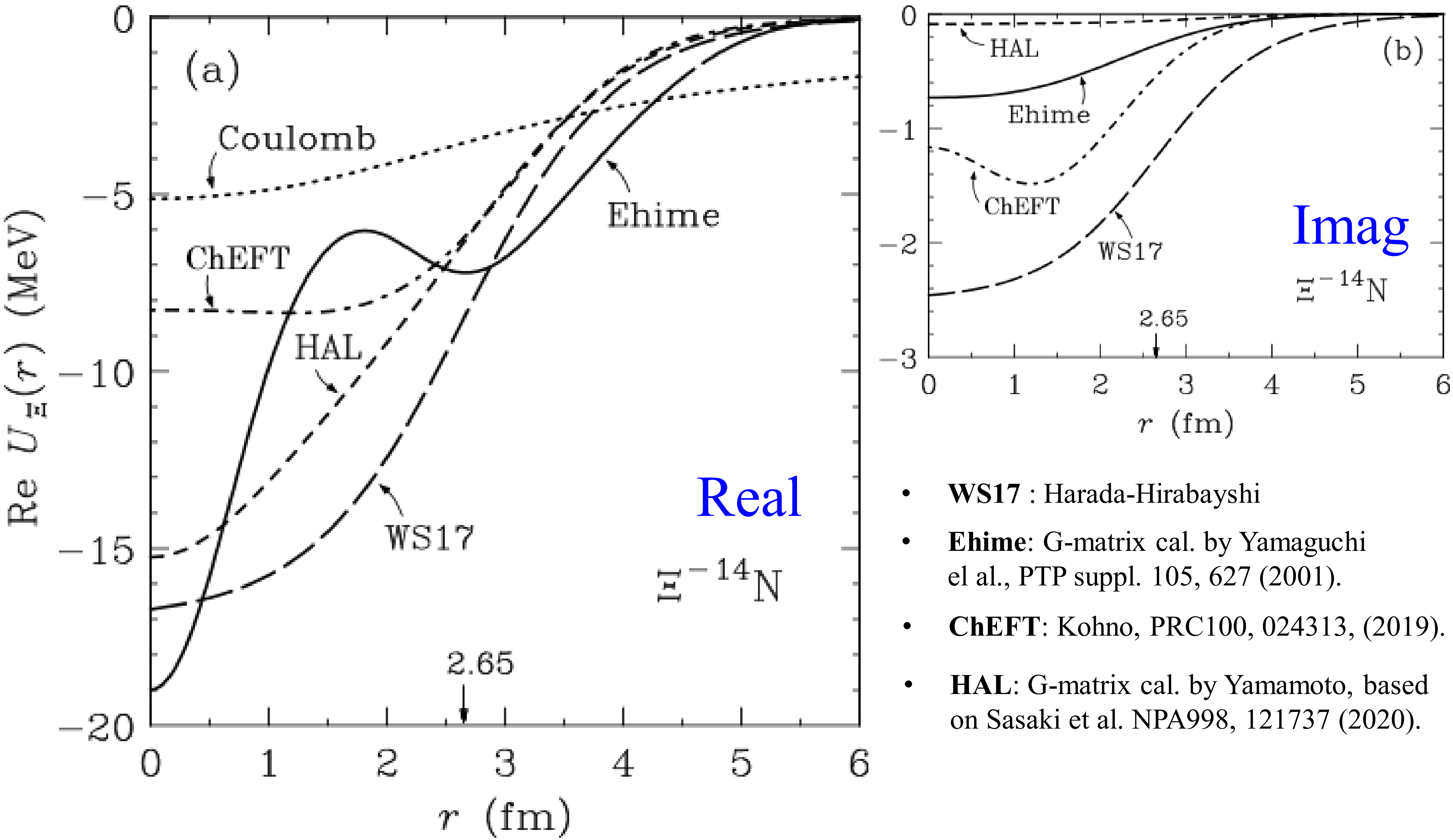

- **WS17** : Harada-Hirabayshi
- **Ehime**: G-matrix cal. by Yamaguchi el al., PTP suppl. 105, 627 (2001).
- **ChEFT**: Kohno, PRC100, 024313, (2019).
- **HAL**: G-matrix cal. by Yamamoto, based on Sasaki et al. NPA998, 121737 (2020).

Ξ-nucleus states in $^{14}N+\Xi^-$

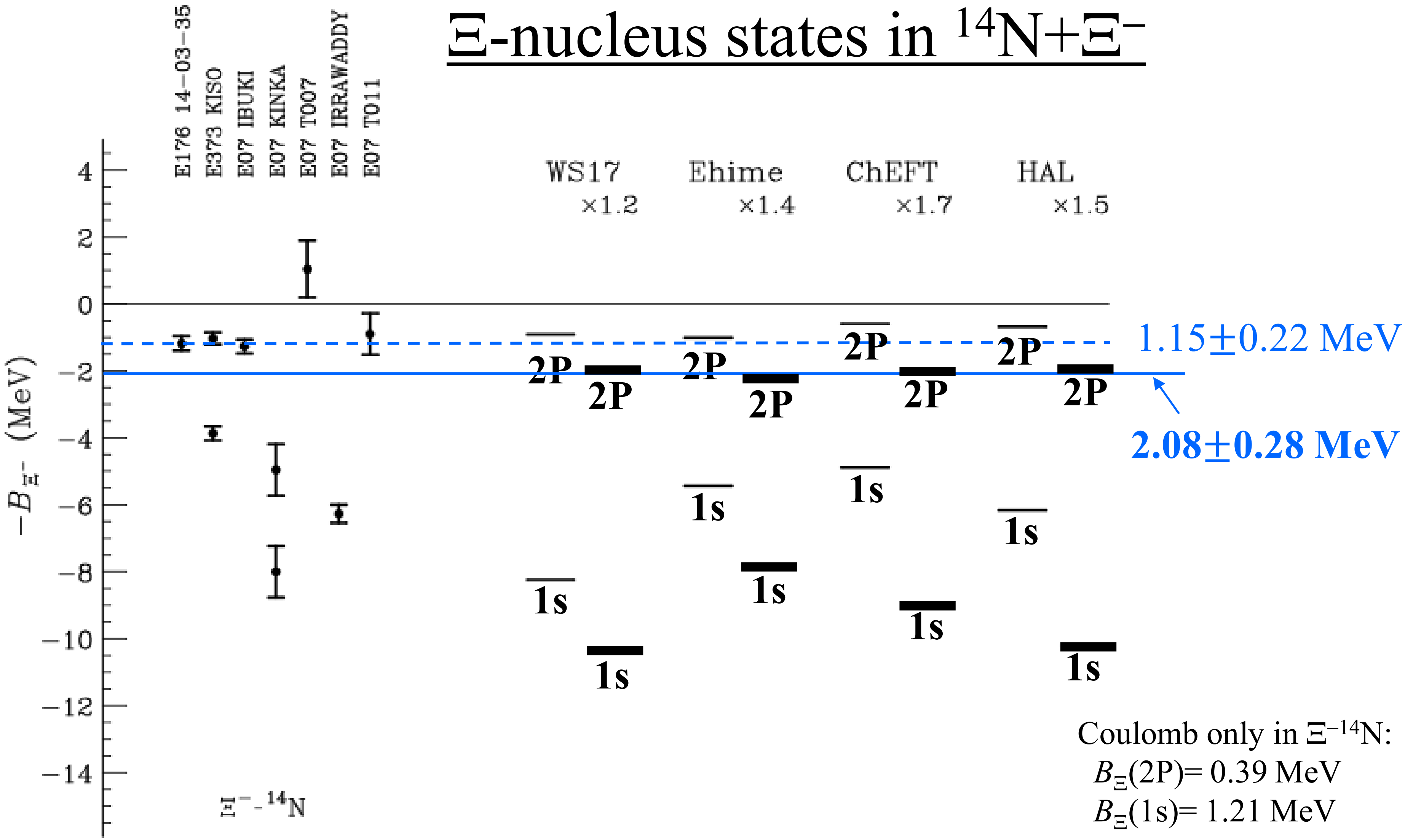

✓ If we try to explain the experimental value of $B_\Xi(2P) = 2$ MeV for ^{14}N-Ξ^- by introducing artificial factors, we need much more attractive in these potentials.

Ξ^--^{56}Fe potentials for Ξ^--atomic states

Ξ^--nucleus optical potentials in $^{56}Fe+\Xi^-$

WS and theoretical potentials by microscopic calculations

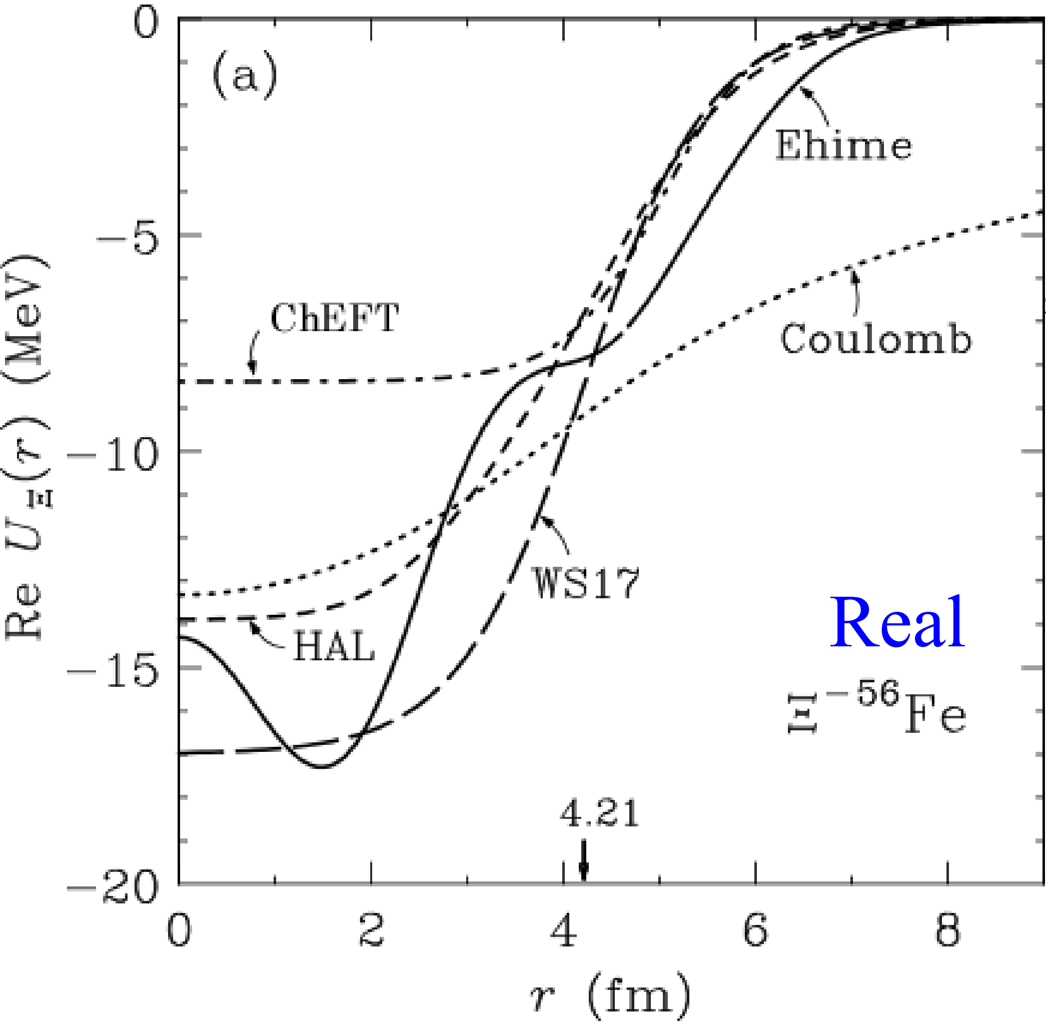

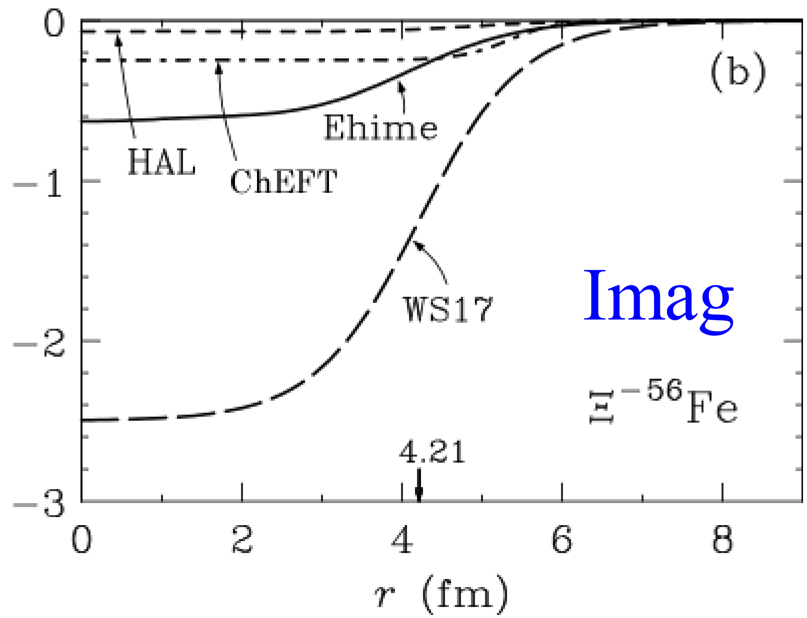

- **WS17** : Harada-Hirabayshi
- **Ehime**: G-matrix cal. by Yamaguchi el al., PTP suppl. 105, 627 (2001).
- **ChEFT**: Kohno-Miyagawa, PTEP 2021, 103D04
- **HAL**: G-matrix cal. by Yamamoto, based on Sasaki et al. NPA998, 121737 (2020).

J-PARC E03: Ξ^- atomic X-ray on ^{56}Fe

Strong-shifts and widths on Ξ^- atoms

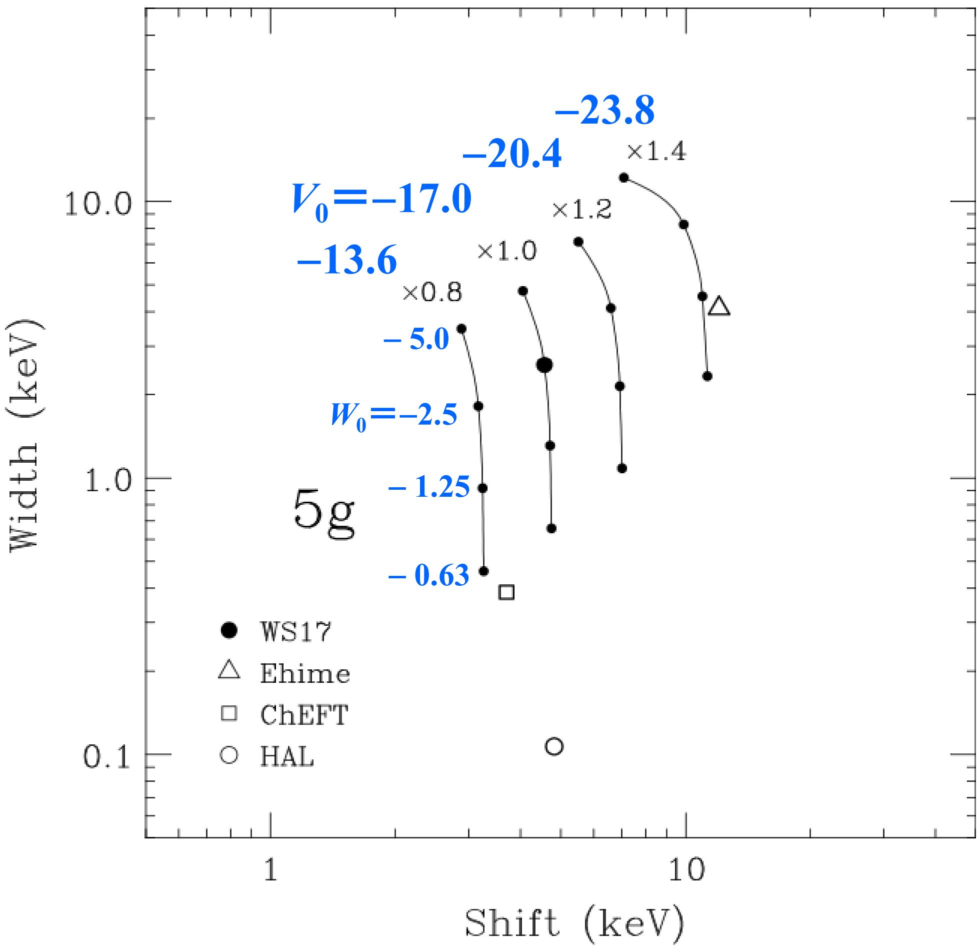

$\Xi^{-56}Fe$

Dependence of V_0 and W_0 :

$V_0 = -13.6, -17.0, -20.4, -23.8$ MeV

$W_0 = -0.63, -1.25, -2.50, -5.00$ MeV

✓ Strong-shifts and widths on Ξ^{-56}Fe indicate useful information on the properties of the Ξ-nucleus potential in the surface region, especially the imaginary parts.

Strong-shifts and widths on Ξ^- atoms

07 Feb. 2022

$\Xi^{-56}Fe$

		5g	6h	
WS17	E	4.565	0.0285	(keV)
	Width	2.564	0.0098	
Ehime	E	12.016	0.0837	
	Width	4.112	0.0086	
ChEFT	E	3.702	0.0207	
	Width	0.386	0.0012	
HAL	E	4.819	0.0337	
	Width	0.107	0.0004	
fss2	E	1.281	0.012	(Kohno)
	Width	0.088	0.001	

Summary

We have discussed theoretically production of Ξ^- hypernuclei in the nuclear (K^-, K^+) reaction and properties of the Ξ-nucleus potentials.

- We have studied the Ξ^- production spectrum of the ^{9}Be(K^-, K^+) reaction at 1.8 GeV/c within the DWIA using the optimal Fermi-averaged $K^- p \to K^+ \Xi^-$ amplitude.

  T. Harada and Y. Hirabayashi, PRC102 (2020) 024618.

- The weak attraction in the Ξ-nucleus potential for Ξ^--^{8}Li provides the ability to explain the BNL-E906 data, consistent with analyses for previous experiments: $V_0 = -17 \pm 6$ MeV for $W_0 = -5$ MeV

  T. Harada and Y. Hirabayashi, PRC103 (2021) 024605.

- We discuss the properties of Ξ-nucleus potentials compared to the recent emulsion data.
- Future subjects and prospects → ΞNN force and ΞN-$\Lambda\Lambda$ coupling

More information on Ξ^- bound states and widths is needed.

Thank you very much for your attention.